

Galactic tide and some properties of the Oort cloud

J. Klačka¹, L. Kómar¹, P. Pástor^{1,2}, M. Jurčí¹, and E. Hönschová¹

¹ Department of Astronomy, Physics of the Earth, and Meteorology
Faculty of Mathematics, Physics and Informatics, Comenius University
Mlynská dolina, 842 48 Bratislava, Slovak Republic
e-mails: klacka@fmph.uniba.sk, komar@fmph.uniba.sk
pavol.pastor@fmph.uniba.sk, jurci@fmph.uniba.sk

² Tekov Astronomical Observatory,
Sokolovská 21, 934 01, Levice, Slovak Republic

Abstract. The paper deals with several properties of the Oort cloud of comets. Sun, Galaxy (and Jupiter) gravitationally act on the comets. New physical model of galactic tide is considered. The main results can be summarized as follows:

1. Mass of the Oort cloud of comets is less than 1 mass of the Earth (M_E), probably not greater than $1/2 M_E$.
2. Theoretical number of long-period comets with perihelion distance $q < 5$ AU is about 50-times greater than the conventional approach yields. Gravity of Jupiter was taken into account in finding this result.
3. Semi-major axis a and period of oscillations P of eccentricity (and other orbital elements) are related as $a^3 P = 1$ in natural units for a moving Solar System in the Galaxy. The natural unit for time is the orbital period of the Solar System revolution around the galactic center and the natural unit for measuring the semi-major axis is its maximum value for the half-radius of the Solar System corresponding to the half-radius of the Oort cloud. The relation holds for the cases when comets approach the inner part of the Solar System, e.g., perihelion distances are less than ≈ 100 AU.
4. The minimum value of semi-major axis for the Oort cloud is $a_{min} \ll 1 \times 10^4$ AU. This condition was obtained both from the numerical results on cometary evolution under the action of the galactic tides and from the observational distribution of long-period comets. If the density function of semi-major axis is approximated by proportionality a^α , then α is $-1/2$, approximately.
5. The magnitude of the change in perihelion distance per orbit, Δq , of a comet due to galactic tides is a strong function of semi-major axis a , proportional to $a^{8.25}$.

Key words. comets, Oort cloud, Galaxy

1. Introduction

Intense modeling of the Oort cloud of comets started practically immediately after the Oort's paper (Oort 1950). As for the current status of the ideas about the Oort cloud we refer to review papers, e.g., Dones et al. (2004), Levison and Jones (2007).

New physical access to the theoretical modeling of the Oort cloud of comets was suggested by Klačka (2009a, 2009b). It is based on a new approach to treating the effect of galactic tides, including improvement of the model of the Galaxy. Its significance was discussed by Kómar et al. (2009). Analytical approach to secular evolution of orbital elements was discussed by Pástor et al. (2009). The aim of this paper is to present some characteristics obtained from the new model. The new model is represented by Eqs. (26)-(27) in Klačka (2009a) and denoted as the Model II in Kómar et al. (2009). The last paper showed the importance of the new model in comparison with the conventional models. Thus, we will not make any calculation based on the conventional models. Instead of that we will concentrate on calculations based on the new modeling of galactic tides. The results of the calculations will be compared with the results obtained by other authors using conventional models of galactic tides.

Sec. 2 deals with distribution of cometary inclinations and it sheds some light also on the value of the exponent α describing distribution of semi-major axes of comets in the Oort cloud. Sec. 3 shows that the magnitude of the change in perihelion distance per orbit of a comet due to galactic tides is a strong function of semi-major axis a , proportional to $a^{8.25}$. Sec. 4 relates the semi-major axis of

a comet and period of oscillation in other orbital elements due to galactic tides. The found relation reminds the third Kepler's law, also in the case when natural units of length and time are used. Secs. 5 and 6 discuss some theoretical access to cometary distributions in eccentricity, perihelion distance and semi-major axis. However, Sec. 6.3 presents also results obtained by numerical integration of equation of motion for comets under the action of the Sun and the Galaxy. Sec. 7 determines minimal perihelion distances q_{min} and inclinations for the instant when q_{min} occurs. The section uses analytical approach to secular time derivatives of orbital elements when the initial cometary inclinations differ from 90° . The two sources of gravity, the Sun and the Galaxy, are used also in Sec. 8 dealing with the distribution of comets in inclination to ecliptic. Sec. 9 improves the most relevant previous results also for the case when the planet Jupiter gravitationally influences the motion of the comets. Finally, Sec. 10 deals with the distribution function in semi-major axis and the number of comets in the Oort cloud, including estimate of the mass of the Oort cloud.

2. Distribution of cometary inclinations

We are interested in distribution function of inclination of comets. The inclination is the angle between a reference plane and the instantaneous orbital plane of a comet.

Probability that a comet has an inclination lying in the interval $(i - di/2, i + di/2)$ is

$$\begin{aligned} dp &= h(i) d\Omega , \\ d\Omega &= 2 \pi \sin i di , \end{aligned} \tag{1}$$

where $d\Omega$ is the solid angle and $h(i)$ is a function, $i \in \langle 0, \pi \rangle$. It is assumed that the normalization condition

$$\begin{aligned} \int_{4\pi} h(i) d\Omega &= 1 , \\ 2 \pi \int_0^\pi h(i) \sin i di &= 1 \end{aligned} \tag{2}$$

holds. The distribution function is

$$\begin{aligned} H(i) &= 2 \pi \int_0^i h(i') \sin i' di' , \\ H(\pi) &= 1 . \end{aligned} \tag{3}$$

The density function is

$$\begin{aligned} h_H(i) &\equiv \frac{dH}{di} = 2 \pi h(i) \sin i . \\ H(\pi) &= 1 . \end{aligned} \tag{4}$$

The mean value is given by relation

$$\langle i \rangle = 2 \pi \int_0^\pi i' h(i') \sin i' di' , \tag{5}$$

The special case of the isotropic distribution is defined by $h(i) = \text{constant}$. Eqs. (3)-(5) reduce to

$$\begin{aligned} H(i) &= \frac{1}{2} (1 - \cos i) , \\ \langle i \rangle &= \frac{\pi}{2} , \\ h_H(i) &= \frac{1}{2} \sin i . \\ h(i) &\equiv \frac{1}{4 \pi} . \end{aligned} \tag{6}$$

Equal numbers of prograde ($i < \pi/2$) and retrograde ($i > \pi/2$) orbits exist.

2.1. Results of orbital evolution – inclination to galactic equator

We are dealing with distribution of comets in the Oort cloud in this subsection. We are interested in the distribution of inclination measured with respect to the galactic equatorial plane.

We made detailed numerical calculations of the orbital evolution of comets under the action of gravity of the Sun and Galaxy (Klačka 2009a, 2009b, Kómar et al. 2009). The results showed that initial inclination of a comet decreased to some value if i_{in} was smaller than 90° and increased to another value if i_{in} was greater than 90° . In reality the inclination changes on a time scale of millions of years. Fig. 1 depicts such kind of evolution of inclination of a comet moving initially on almost circular orbit in a distance of 5.0×10^4 AU. We are interested in time average of the inclination in order to find results comparable with statements presented in literature (e.g., Duncan et al. 1987, Bailey 1983, Fernández and Ip 1987, Fernández 1992, Fernández and Gallardo 1999).

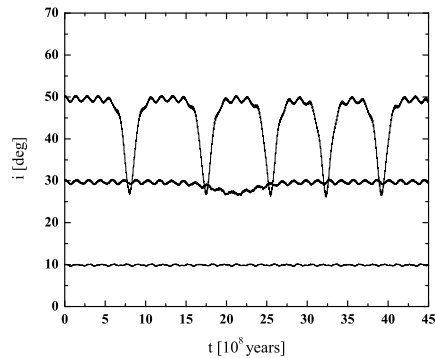


Fig. 1. Time evolution of inclination of a comet moving initially on almost circular orbit in a distance of 5.0×10^4 AU. Three initial values of inclination are considered.

Table 1 presents the averaged time values of a comet with a given initial inclination. On the basis of the data presented in Table 1 we can conclude that the function $h(i)$ is not a constant. E.g, the interval $i_{in} \in \langle 70^\circ, 90^\circ \rangle$ produces the time averaged values $i \in \langle 60^\circ, 90^\circ \rangle$. An approximation yields that for a mean value $i[\text{deg}] \approx 60 + (90 - 60)/2 = 75$ the following value holds: $h(75^\circ) \approx (90 - 70)/(90 - 60)/(4\pi) = 2/3/(4\pi)$. Similarly, the interval $i_{in} \in \langle 25^\circ, 70^\circ \rangle$ produces the time averaged values $i \in \langle 25^\circ, 60^\circ \rangle$. An approximation yields that for a mean value $i[\text{deg}] \approx 25 + (60 - 25)/2 = 42.5$ the following value holds: $h(42.5^\circ) \approx (70 - 25)/(60 - 25)/(4\pi) \approx 4/3/(4\pi)$. Thus, we can conclude that $h(\pi/4) \approx (4/3)(4\pi)^{-1}$. One can see the difference between the value and the result presented in Eqs. (6). The result $h(\pi/4) \approx (4/3)(4\pi)^{-1}$ holds for semi-major axis $a = 5.0 \times 10^4$ AU. The smaller a , the closer the result to that given in Eq. (6).

i_{in}	i	i_{in}	i
[deg]	[deg]	[deg]	[deg]
0.00	0.00	90.00	89.47
10.00	9.89	110.00	119.72
30.00	29.31	130.00	134.88
50.00	45.12	150.00	150.69
70.00	60.28	180.00	180.00

Table 1. Values of time averaged inclination i for a comet with a given initial inclination i_{in} for initially almost circular orbit and semi-major axis $a = 5.0 \times 10^4$ AU due to the galactic tide.

Detailed numerical calculations show that the function h defined by Eqs. (1) depends not only on the inclination i , but also on the semi-major axis a . The most relevant results are presented in Table

2. The function for $a = 2.5 \times 10^4$ AU is depicted in Fig. 2, where also isotropic function is shown, for comparison.

a	i_{max}	$h(i_{max}, a) / h(i=0, a)$
[10^4 AU]	[rad]	—
$\rightarrow 0.0$	$\langle 0, \pi/2 \rangle$	1.0
2.5	$0.71 \times \pi/4$	1.5
5.0	$0.87 \times \pi/4$	1.5

Table 2. Maxima of the function $h(i, a)$, $h_{max} = h(i_{max}, a)$, for various values of cometary semi-major axes a . The maximum of h holds for the angle i_{max} . The interval $i \in \langle 0, \pi/2 \rangle$ is considered.

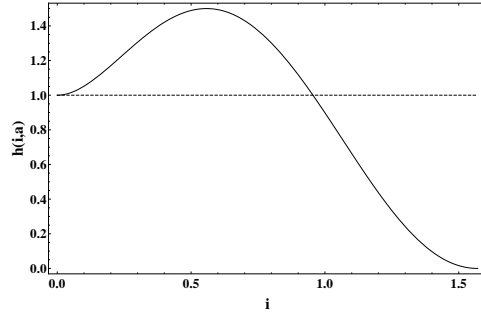


Fig. 2. Function of inclination with respect to the galactic equatorial plane. The solid line holds for the gravity of the Galaxy and the Sun and for the semi-major axis $a = 2.5 \times 10^4$ AU. The dotted line corresponds to the two-body problem.

The function can be approximated by the following conditions:

$$\begin{aligned}
 \lim_{i \rightarrow 0} \frac{\partial h(i, a)}{\partial i} &= 0, \\
 h\left(\frac{\pi}{2}, a\right) &= 0, \\
 \lim_{i \rightarrow \pi/2} \frac{\partial h(i, a)}{\partial i} &= 0, \\
 i = i_{max} : h(i_{max}, a) &= \max \left\{ h(i, a), i \in \langle 0, \frac{\pi}{2} \rangle \right\}, \\
 \lim_{i \rightarrow i_{max}} \frac{\partial h(i, a)}{\partial i} &= 0.
 \end{aligned} \tag{7}$$

Moreover,

$$\begin{aligned}
 h\left(\frac{\pi}{2} + i, a\right) &= h\left(\frac{\pi}{2} - i, a\right), \\
 i &\in \langle 0, \frac{\pi}{2} \rangle.
 \end{aligned} \tag{8}$$

On the basis of the values presented in Table 2 and Eqs. (7) we can make the following approximation

$$\begin{aligned}
 h(i, a) &= h_a(i) \times (1 + i + c_{12} a i^2 + c_{22} a^2 i^2 + c_{13} a i^3 + c_{23} a^2 i^3), \\
 h_a(i) &= \left(2 - \frac{\pi}{2}\right) \left(\frac{2}{\pi}\right)^3 i^3 + (\pi - 3) \left(\frac{2}{\pi}\right)^2 i^2 - i + 1, \\
 c_{12} &= + 4.89184,
 \end{aligned}$$

$$\begin{aligned}
c_{22} &= -0.80376, \\
c_{13} &= -3.23854, \\
c_{23} &= +0.67758.
\end{aligned} \tag{9}$$

The function independent of semi-major axis is

$$\begin{aligned}
h(i) &\propto \frac{\int_{a_{min}}^{a_{max}} a^\alpha h(i, a) da}{\int_{a_{min}}^{a_{max}} a^\alpha da}, \\
\alpha &\in (-4, -2); -3/2; \dots.
\end{aligned} \tag{10}$$

We inserted also the values of the exponent α taken from Fernández and Gallardo (1999), Duncan et al. (1987). We finally obtain

$$\begin{aligned}
h(i) &= Kh_a(i) \left[1 + i - \frac{\ln\left(\frac{a_{max}}{a_{min}}\right)}{a_{max}^{-1} - a_{min}^{-1}} C_1(i) - \frac{a_{max} - a_{min}}{a_{max}^{-1} - a_{min}^{-1}} C_2(i) \right], \quad \alpha = -2, \\
h(i) &= Kh_a(i) \left[1 + i + 2 \frac{a_{max}^{-1} - a_{min}^{-1}}{a_{max}^{-2} - a_{min}^{-2}} C_1(i) - 2 \frac{\ln\left(\frac{a_{max}}{a_{min}}\right)}{a_{max}^{-2} - a_{min}^{-2}} C_2(i) \right], \quad \alpha = -3, \\
h(i) &= Kh_a(i) \left[1 + i + \frac{\alpha + 1}{\alpha + 2} \frac{a_{max}^{\alpha+2} - a_{min}^{\alpha+2}}{a_{max}^{\alpha+1} - a_{min}^{\alpha+1}} C_1(i) + \frac{\alpha + 1}{\alpha + 3} \frac{a_{max}^{\alpha+3} - a_{min}^{\alpha+3}}{a_{max}^{\alpha+1} - a_{min}^{\alpha+1}} C_2(i) \right], \\
\alpha &\in (-4, -3) \cup (-3, -2); -3/2; \dots, \\
C_1(i) &= c_{12} i^2 + c_{13} i^3, \\
C_2(i) &= c_{22} i^2 + c_{23} i^3,
\end{aligned} \tag{11}$$

The quantity $K \equiv K(\alpha, a_{min}, a_{max})$ is determined by the normalization condition

$$2\pi \int_0^\pi h(i, \alpha, a_{min}, a_{max}) \sin i \, di = 1. \tag{12}$$

Having the function defined by Eqs. (11)-(12), we can find the distribution function defined by Eq. (3) and the observational mean value $\langle i \rangle$. It follows

$$\langle i \rangle = \frac{\pi}{2}. \tag{13}$$

Our detailed numerical calculations considering tidal effect of Galaxy show that amplitude of semi-major axis a rapidly increases with the value of a when $a > 5 \times 10^4$ AU. If $a = 7.5 \times 10^4$ AU, then the amplitude of oscillation is 5×10^3 AU. Moreover, if a is comparable with 1×10^5 AU, then an increase of semi-major axis exists. More correctly, there does not exist a constant value of semi-major axis for secular evolution, an amplitude is about 25×10^3 AU. Thus, the effect of galactic tide causes that stability of the Oort cloud exists only for $a < a_{max}$ and $a_{max} \approx 0.8 \times 10^5$ AU. This seems to be consistent with observations, according to which $a_{max} \approx 1 \times 10^5$ AU and $a_{min} \approx 1 \times 10^4$ AU (see also Fig. 1 in Fernández 1992), although the value $a_{min} = 1.5 \times 10^4$ AU is also presented (Fernández and Ip 1987).

Fig. 3 depicts the function(s) $h(i)$. Although the presented curves do not exhibit any significant difference, the real results are relevant. At first, if we take into account $a_{min} \rightarrow 0$, more correctly $a_{min} \ll 1 \times 10^4$ AU, then various values of α can be used and the function practically does not depend on the real value of α . The value $a_{min} \rightarrow 0$ is consistent with the data obtained from observational data on long-period comets (see Sec. 10), but it is not consistent with the conventional statements discussed in the previous paragraph. However, if we would like to use the values not fulfilling $a_{min} \rightarrow 0$, e.g., $a_{min} = 1.0 \times 10^4$ AU or $a_{min} = 2.0 \times 10^4$ AU, then the only acceptable value of α is -1 : the value $\alpha \neq -1$ would produce nonpositive function h . The value $\alpha = -1$ is not consistent with the

conventional statements on the Oort cloud that $\alpha = -3/2$ or $\alpha \in (-4, -2)$ (Duncan et al. 1987, Bailey 1983, Fernández and Ip 1987, Fernández 1992, Fernández and Gallardo 1999). Moreover, the observational data suggest that α is closer to zero: $\alpha = 0.13$ (see Eqs. 74 in Sec. 10), or $\alpha = -0.55$ (see Eqs. 76 in Sec. 10).

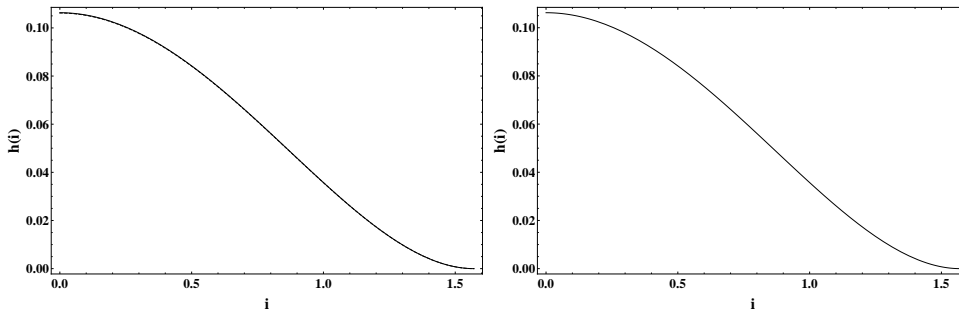


Fig. 3. The function of inclination with respect to the galactic equatorial plane $h(i)$. Averaging over distribution in semi-major axis is done. The upper/left part of the figure is characterized by the values $a_{min} \rightarrow 0$, $a_{max} = 10 \times 10^4$ AU (practically independent of α). The lower/right part of the figure corresponds to the case $a_{min} = 1 \times 10^4$ AU, $a_{max} = 10 \times 10^4$ AU and $\alpha = -1.0$.

3. Timescales on which a comet's perihelion changes

A formula for a timescales on which a comet's perihelion changes is presented by Levison and Dones (2007, p. 583). However, as it is discussed by Kómar et al. (2009), the formula does not correspond to reality. It is important to find mathematical relation(s) which are based on physical approach.

In order to obtain the cases when comets approach the inner part of the Solar System, e.g., perihelion distances are less than ≈ 100 AU, we consider initial inclinations with respect to the galactic equatorial plane about 90 degrees.

3.1. First approach

Let us consider the change of perihelion distance per revolution of a comet around the Sun. The period of revolution of the comet is T [years], the change of perihelion distance during the period T is Δq [AU] and semi-major axis of the comet is a [AU]. Fig. 4 holds for the cases when q obtains its minimum values during the time evolution $q(t)$ for 4.5×10^9 years. The solid line is an analytical approximation to numerical results obtained from evolution for the model of Klačka (2009a, Eqs. 26-27; Model II in Kómar et al. 2009). We can conclude that

$$\begin{aligned} \log_{10} \left(\frac{\Delta q}{T} \right) &= A_1 + A_2 \log_{10} a, \\ A_1 &= -35.95 \pm 0.89, \\ A_2 &= +6.75 \pm 0.20. \end{aligned} \tag{14}$$

3.2. Second approach

We want to find a formula which is more similar to the mathematical formula presented by Levison and Dones (2007, p. 583). As it was already stressed, our formula must respect physical reality. We can use detailed numerical calculation for orbital evolution for our new model (Klačka 2009a, 2009b; Model II in Kómar et al. 2009), or we can try to use the analytical approach to secular evolution of orbital elements (discussed by Pástor et al. 2009). The analytical approach is limited by the condition that semi-major axis of a comet must be less than about 1.5×10^4 AU if the condition $T \times (1/T_z +$

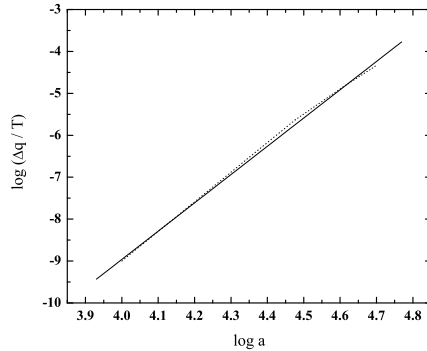


Fig. 4. Change of perihelion distance Δq [AU] per revolution of a comet around the Sun. The period of revolution of the comet is T [years] and semi-major axis of the comet is a [AU]. Solid line corresponds to linear fit of the numerical solution (dashed curve) for the tidal effect of the Galaxy.

$1 / T_0) < 0.05$, where T_z is the period of oscillations of the Sun with respect to the galactic equatorial plane and T_0 is the period of revolution of the Sun with respect to the center of the Galaxy.

Detailed solution of the equation of motion corresponding to Model II yields

$$\log_{10} \left(\frac{\Delta q}{T} \right) = A_1 + A_2 \log_{10} a + A_3 \log_{10} q ,$$

$$\begin{aligned} A_1 &= - 33.67 \pm 1.48 , \\ A_2 &= + 6.29 \pm 0.31 , \\ A_3 &= - 0.12 \pm 0.07 . \end{aligned} \tag{15}$$

Again, as in the previous subsection, the period of revolution of the comet is T [years], the change of perihelion distance during the period T is Δq [AU] and semi-major axis and perihelion distance of the comet are a [AU] and q [AU]. Eqs. (15) contain the same quantities as the relation presented by Levison and Dones (2007, p. 583). It is immediately seen that the values of A_2 and A_3 significantly differ from the values presented by Levison and Dones.

3.3. Comparison of the approaches

We have found two relations, one of them is represented by Eqs. (14), the other one by Eqs. (15). None of them is consistent with the relation presented by Levison and Dones (2007, p. 583). Moreover, the relation represented by Eqs. (15) is characterized by much greater errors of the coefficients than it is in the case of Eqs. (14).

Secular approach to the orbital evolution treated by Pástor et al. (2009) also confirms that the relation presented by Levison and Dones (2007, p. 583) is not consistent with physics of the galactic tide.

According to Eqs. (14)-(15) we see that the magnitude of the change in perihelion distance per orbit, Δq , of a comet due to galactic tides is a strong function of semi-major axis a , proportional to $a^{8.25}$, or considering some error, a^δ , $\delta \in (7.5, 8.5)$. This is a new result, not consistent with the conventional value $\delta = 3.5$ (see, e.g., Dones et al. 2004, p. 155).

4. Relation between semi-major axis and oscillation period

Galactic tide causes oscillations of eccentricity (perihelion and aphelion distances, angular orbital elements) of a comet in the Oort cloud (see Fig. 7 in Kómar et al. 2009). We are interested in a relation between the semi-major axis a and the oscillation period P of the comet.

We are interested in the cases when comets approach the inner part of the Solar System, e.g., perihelion distances are less than ≈ 100 AU. Thus, we consider the values of about 90 degrees for

the initial inclinations with respect to the galactic equatorial plane. Various values of other orbital elements are taken into account.

Detailed numerical calculations for $1 \times 10^4 \text{ AU} < a < 8 \times 10^4 \text{ AU}$ yield the result presented in Fig. 5, which yields

$$\begin{aligned} \log_{10} a &= A \log_{10} P + B , \\ A &= -0.362 \pm 0.029 , \\ B &= +7.846 \pm 0.254 , \\ [a] &= \text{AU} , \quad [P] = \text{yr} . \end{aligned} \tag{16}$$

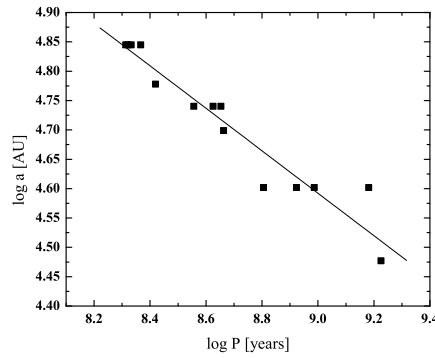


Fig. 5. Semi-major axis a as a function of oscillation period P of eccentricity of a comet from the Oort cloud. The oscillations are caused by the effect of galactic tide. Solid line corresponds to linear fit of the data obtained by numerical solution for the tidal effect of the Galaxy. The data for initial inclination 90 degrees are used (other values of inclinations may yield a little different values).

Since the period of oscillations slightly changes on the scales of billions of years, we can rewrite Eq. (16) into a more simple relation $a^3 P = \text{constant}$. The value of the *constant* is determined by the least square method. We obtain

$$\begin{aligned} a^3 P &= \text{constant} , \\ \text{constant} &= (6.93 \pm 0.23) \times 10^{22} \text{AU}^3 \text{ yr} , \\ [a] &= \text{AU} , \quad [P] = \text{yr} . \end{aligned} \tag{17}$$

In natural units for the moving Solar System in the Galaxy we obtain

$$a^3 P = 1 . \tag{18}$$

The natural unit for time is the orbital period of Solar System revolution around the galactic center, $2\pi/(A - B) = 2.3 \times 10^8 \text{ yrs}$. The natural unit for the semi-major axis is its maximum value for the half-radius of the Solar System which equals to the half-radius of the Oort cloud, $0.7 \times 10^5 \text{ AU}$. The value yields limiting cometary aphelion distances $1.4 \times 10^5 \text{ AU}$, half of the distance between the Sun and its nearest star.

As a first approximation, a comet of the Oort cloud revolves around the Sun on an ellipse fulfilling the third Kepler's law $a^3/T^2 = \text{constant}(\text{two body problem})$, where T is period of revolution of the comet. Moreover, eccentricity of the comet oscillates due to the effect of galactic tide and the period of oscillations of the eccentricity relates the semi-major axis of the comet as $a^3 P = \text{constant}(\text{galactic tide})$.

5. Probability that eccentricity is less than a given value

We are interested in the probability $P(e < e_L)$ that eccentricity e of comets is less than a given value e_L .

Orbital evolution of eccentricity due to the effect of galactic tides is a periodic function of time, approximately. We will use the following approximation:

$$\begin{aligned} e(t) &= \frac{1}{2} \left\{ 1 - \sin \left[\frac{\pi}{2} \left(4 \frac{t}{P} - \delta_{in} \right) \right] \right\} , \\ e(t=0) &\equiv e_{in} = \frac{1}{2} \left[1 + \sin \left(\frac{\pi}{2} \delta_{in} \right) \right] , \\ \delta_{in} &= \frac{2}{\pi} \arcsin(2e_{in} - 1) , \\ \delta_{in} &\in \langle -1, +1 \rangle , \quad e_{in} \in \langle 0, +1 \rangle , \end{aligned} \quad (19)$$

for the time evolution of eccentricity $e(t)$ with the period of oscillations P , as it is discussed in the previous section.

5.1. Density and distribution functions of eccentricity

Let an initial distribution of eccentricities of comets in the Oort cloud is represented by a density function $f(e_{in})$. We are interested in the density function $f(e)$ at a given time t . We have $e = e(t)$, $e(t=0) = e_{in}$. Gravitation of the Sun and Galaxy will be considered.

If F is the distribution function, then

$$\begin{aligned} dF &= f[e(t)] de , \\ dF &= f(e_{in}) de_{in} . \end{aligned} \quad (20)$$

Knowing the inverse function $e_{in} = g^{-1}(e)$ to the function $g(e_{in})$, Eqs. (20) yield

$$f(e) = f[g^{-1}(e)] \frac{1}{|g'[g^{-1}(e)]|} . \quad (21)$$

Let us rewrite Eq. (19) into the form

$$e = g(e_{in}) = \frac{1}{2} \left[1 - 2 \sin \left(\frac{2\pi t}{P} \right) \sqrt{e_{in}(1 - e_{in})} + \cos \left(\frac{2\pi t}{P} \right) (2e_{in} - 1) \right] . \quad (22)$$

Since this function is not monotonous, its inverse function does not exist. However, it is possible to split the function $g(e_{in})$ into two monotonous functions. There exist inverse functions for the two monotonous functions:

$$\begin{aligned} g^{-1}(e) &= - \sqrt{e(1 - e)} \left| \sin \left(\frac{2\pi t}{P} \right) \right| + \frac{1}{2} \left[1 + (2e - 1) \cos \left(\frac{2\pi t}{P} \right) \right] , \\ e_{in} &\in \langle 0, \sin^2 \left(\frac{\pi t}{P} \right) \rangle , \end{aligned} \quad (23)$$

and

$$\begin{aligned} g^{-1}(e) &= + \sqrt{e(1 - e)} \left| \sin \left(\frac{2\pi t}{P} \right) \right| + \frac{1}{2} \left[1 + (2e - 1) \cos \left(\frac{2\pi t}{P} \right) \right] , \\ e_{in} &\in \langle \sin^2 \left(\frac{\pi t}{P} \right), 1 \rangle . \end{aligned} \quad (24)$$

Eqs. (21), (23)-(24) yield

$$f(e) = f[g^{-1}(e)] \frac{1}{|\cos \chi + X_{e1}|} ,$$

$$\begin{aligned}
X_{e1} &= \frac{(2e-1) \cos \chi \sin \chi - 2\sqrt{e(1-e)} |\sin \chi| \sin \chi}{\sqrt{1 + [1 + 8e(e-1)] \sin^2 \chi - (2e-1)^2 + 4(2e-1)\sqrt{e(1-e)} |\sin \chi| \cos \chi}}, \\
e_{in} &= g^{-1}(e) = -\sqrt{e(1-e)} |\sin \chi| + \frac{1}{2} [1 + (2e-1) \cos \chi], \\
\chi &= \frac{2\pi}{P} t, \\
e_{in} &\in \langle 0, \sin^2 \left(\frac{\pi t}{P} \right) \rangle,
\end{aligned} \tag{25}$$

and,

$$\begin{aligned}
f(e) &= f[g^{-1}(e)] \frac{1}{|\cos \chi + X_{e2}|}, \\
X_{e2} &= \frac{(2e-1) \cos \chi \sin \chi + 2\sqrt{e(1-e)} \sin^2 \chi}{\sqrt{1 + [1 + 8e(e-1)] \sin^2 \chi - (2e-1)^2 - 4(2e-1)\sqrt{e(1-e)} |\sin \chi| \cos \chi}}, \\
e_{in} &= g^{-1}(e) = +\sqrt{e(1-e)} |\sin \chi| + \frac{1}{2} [1 + (2e-1) \cos \chi], \\
\chi &= \frac{2\pi}{P} t, \\
e_{in} &\in \langle \sin^2 \left(\frac{\pi t}{P} \right), 1 \rangle.
\end{aligned} \tag{26}$$

The distribution function is

$$\begin{aligned}
F(e) &= \int_0^e f(e') de', \\
F(1) &= 1.
\end{aligned} \tag{27}$$

We may introduce that instead of Eqs. (20) an alternative approach can be used. Knowing the density function $f(e_{in})$ and $e = g(e_{in})$, we may use a convolution for finding the density function $f(e)$. The convolution yields

$$f(e) = \int f(e_{in}) \delta[e - g(e_{in})] de_{in}. \tag{28}$$

5.1.1. Uniform distribution

Let us consider, as an example, a uniform distribution of eccentricities. The density function is

$$f(e_{in}) = 1, \quad e_{in} \in \langle 0, 1 \rangle. \tag{29}$$

The distribution function is $F(e_{in}) = \int_0^{e_{in}} f(e'_{in}) de'_{in} = e_{in}$, $F(1) = 1$.

Using Eqs. (25)-(26), we obtain

$$\begin{aligned}
f(e) &= \frac{1}{|\cos \chi + X_{e1}|}, \\
X_{e1} &= \frac{(2e-1) \cos \chi \sin \chi - 2\sqrt{e(1-e)} |\sin \chi| \sin \chi}{\sqrt{1 + [1 + 8e(e-1)] \sin^2 \chi - (2e-1)^2 + 4(2e-1)\sqrt{e(1-e)} |\sin \chi| \cos \chi}}, \\
\chi &= \frac{2\pi}{P} t, \\
e_{in} &\in \langle 0, \sin^2 \left(\frac{\pi t}{P} \right) \rangle,
\end{aligned} \tag{30}$$

and,

$$\begin{aligned}
f(e) &= f[g^{-1}(e)] \frac{1}{|\cos \chi + X_{e2}|}, \\
X_{e2} &= \frac{(2e-1) \cos \chi \sin \chi + 2\sqrt{e(1-e)} \sin^2 \chi}{\sqrt{1 + [1 + 8e(e-1)] \sin^2 \chi - (2e-1)^2 - 4(2e-1)\sqrt{e(1-e)} |\sin \chi| \cos \chi}}, \\
\chi &= \frac{2\pi}{P} t, \\
e_{in} &\in \langle \sin^2 \left(\frac{\pi t}{P} \right), 1 \rangle.
\end{aligned} \tag{31}$$

As an illustration we take $t = P/2$. Eqs. (30)-(31) yield $f(e) = 1$, and, the distribution function is $F(e) = e$:

$$\begin{aligned}
f(e) &= 1, \quad t = 0, \\
F(e) &= e, \quad t = 0, \\
f(e) &= 1, \quad t = P/2, \\
F(e) &= e, \quad t = P/2.
\end{aligned} \tag{32}$$

5.1.2. Distribution function $F(e_{in}) = e_{in}^2$

We will consider, as an another example, $F(e_{in}) = e_{in}^2$. Motivation for this distribution function comes from Fernández and Gallardo (1999), Hills (1981) and Jeans (1919). The corresponding density function is

$$f(e_{in}) = 2 e_{in}, \quad e_{in} \in \langle 0, 1 \rangle. \tag{33}$$

Using Eqs. (25)-(26), we obtain

$$\begin{aligned}
f(e) &= \frac{1 + (2e-1) \cos \chi - 2\sqrt{e(1-e)} |\sin \chi|}{|\cos \chi + X_{e1}|}, \\
X_{e1} &= \frac{(2e-1) \cos \chi \sin \chi - 2\sqrt{e(1-e)} |\sin \chi| \sin \chi}{\sqrt{1 + [1 + 8e(e-1)] \sin^2 \chi - (2e-1)^2 + 4(2e-1)\sqrt{e(1-e)} |\sin \chi| \cos \chi}}, \\
\chi &= \frac{2\pi}{P} t, \\
e_{in} &\in \langle 0, \sin^2 \left(\frac{\pi t}{P} \right) \rangle,
\end{aligned} \tag{34}$$

and,

$$\begin{aligned}
f(e) &= \frac{1 + (2e-1) \cos \chi + 2\sqrt{e(1-e)} |\sin \chi|}{|\cos \chi + X_{e2}|}, \\
X_{e2} &= \frac{(2e-1) \cos \chi \sin \chi + 2\sqrt{e(1-e)} \sin^2 \chi}{\sqrt{1 + [1 + 5e(e-1)] |\sin \chi| \sin \chi - (2e-1)^2 - 2(2e-1)\sqrt{e(1-e)} |\sin \chi| \cos \chi}}, \\
\chi &= \frac{2\pi}{P} t, \\
e_{in} &\in \langle \sin^2 \left(\frac{\pi t}{P} \right), 1 \rangle.
\end{aligned} \tag{35}$$

As an illustration we take $t = P/2$. Eqs. (34)-(35) yield $f(e) = 2(1-e)$, and, the distribution function is $F(e) = e(2-e)$:

$$f(e) = e, \quad t = 0,$$

$$\begin{aligned}
F(e) &= \frac{1}{2} e^2, \quad t = 0, \\
f(e) &= 2(1 - e), \quad t = P/2, \\
F(e) &= e(2 - e), \quad t = P/2.
\end{aligned}
\tag{36}$$

The situation represented by Eqs. (36) is illustrated in Fig. 6.

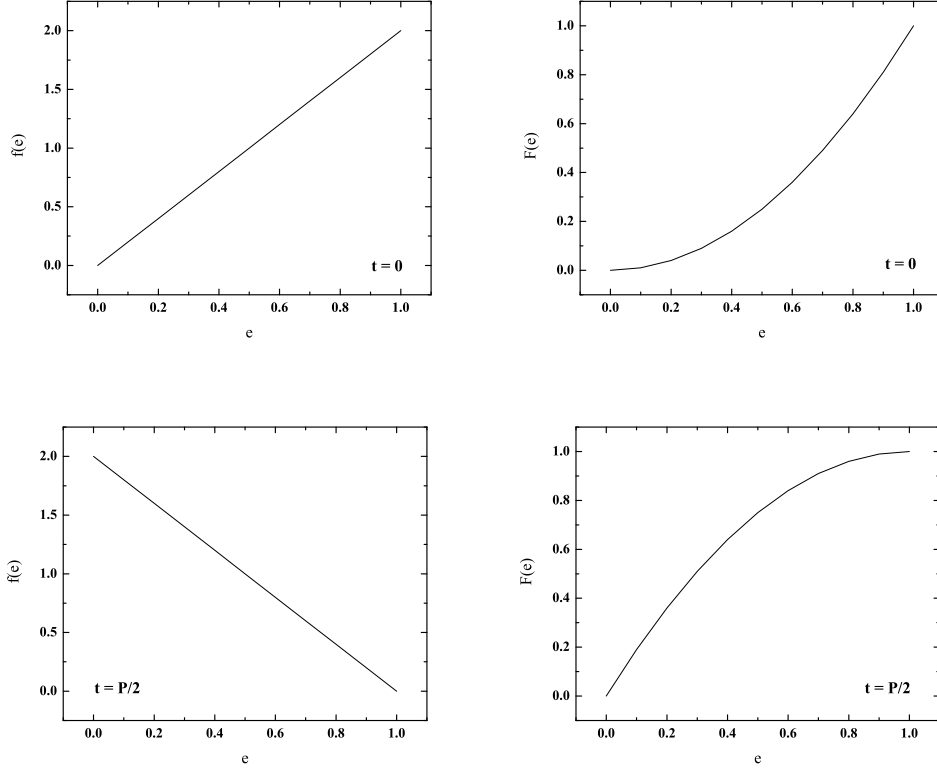


Fig. 6. Density $f(e)$ and distribution $F(e)$ functions of eccentricity for two instants: $t = 0$ and $t = P/2$, where P is the oscillation period of eccentricities (perihelion and aphelion distances, inclinations, ...). The oscillations are caused by the effect of galactic tide.

5.2. $P(e < e_L)$ for a random time

Now, we want to take into account some other important facts. At first, we do not know at which time a given distribution $f(e_{in})$ holds. Then, we know from the previous section that there is a relation between the semi-major axis a and period of oscillations P . Thus, comets with various values of a are characterized with various values of P . Moreover, we do not know the exact value of the parameter α defining the distribution in semi-major axis, as it is presented in Sec. 2. All these facts lead us to the conclusion that we have to find another possibility of obtaining the probability $P(e < e_L)$ that eccentricity of comets e is less than a given value e_L .

Let us consider Eqs. (19). We can write

$$\begin{aligned}
P(e < e_L) &= \frac{\Delta t_L}{P}, \\
\Delta t_L &= |t_{L1} - t_{L2}|,
\end{aligned}$$

$$e_L = \frac{1}{2} \left\{ 1 - \sin \left[\frac{\pi}{2} \left(4 \frac{t_L}{P} - \delta_{in} \right) \right] \right\} . \quad (37)$$

The last equation for e_L determines the two values t_{L1} and t_{L2} . Thus, we finally obtain

$$P(e < e_L) = \frac{1}{2} - \frac{1}{\pi} \arcsin(1 - 2e_L) . \quad (38)$$

6. Probability that perihelion distance is less than a given value

We are interested in the probability $P(q < q_L)$ that perihelion distance q of comets is less than a given value q_L . We will assume that all comets have the same semi-major axis a . Sec. 6.4 will consider joint/cumulative distribution function consisting of two marginal distributions, one in a and another one in q .

Let the orbital evolution of eccentricity due to the effect of galactic tides is given by Eqs. (19). Since $q = a(1 - e)$, Eqs. (19) yield

$$q = \frac{1}{2} a \left[1 + 2 \sin \left(\frac{2\pi t}{P} \right) \sqrt{e_{in}(1 - e_{in})} - \cos \left(\frac{2\pi t}{P} \right) (2e_{in} - 1) \right] . \quad (39)$$

6.1. Distribution and density functions of perihelion distance

We are interested in the probability $P(q < q_L)$ that a perihelion distance q is less than a given value q_L . Since $q = a(1 - e)$ and semi-major axis a is a constant in secular evolution, we immediately obtain $P(q < q_L) = P(e > e_L)$. Thus,

$$\begin{aligned} P(q < q_L) &= 1 - P(e < e_L) , \\ F_q(q) &= 1 - F(e) , \\ P(q < q_L) &= F_q(q_L) , \\ e &= 1 - \frac{q}{a} , \\ q &\in \langle 0, a \rangle , \end{aligned} \quad (40)$$

where F_q is the distribution function of perihelion distance.

The density function $f_q(q)$ of perihelion distance q is, on the basis of Eqs. (40),

$$\begin{aligned} f_q(q) dq &= -f(e) de , \\ f_q(q) &= \frac{1}{a} f(e) , \\ e &= 1 - \frac{q}{a} , \\ q &\in \langle 0, a \rangle . \end{aligned} \quad (41)$$

Eqs. (25)-(26) and Eqs. (41) yield for the density function $f_q(q)$:

$$\begin{aligned} f_q(q) &= \frac{1}{a} f(e) , \quad q \in \langle 0, a \rangle , \\ f(e) &= f[g^{-1}(e)] \frac{1}{|\cos \chi + X_{e1}|} , \\ X_{e1} &= \frac{(2e - 1) \cos \chi \sin \chi - 2\sqrt{e(1 - e)} |\sin \chi| \sin \chi}{\sqrt{1 + [1 + 8e(e - 1)] \sin^2 \chi - (2e - 1)^2 + 4(2e - 1)\sqrt{e(1 - e)} |\sin \chi| \cos \chi}} , \\ e_{in} &= g^{-1}(e) = -\sqrt{e(1 - e)} |\sin \chi| + \frac{1}{2} [1 + (2e - 1) \cos \chi] , \\ e &= 1 - \frac{q}{a} , \\ \chi &= \frac{2\pi}{P} t , \\ e_{in} &\in \langle 0, \sin^2 \left(\frac{\pi t}{P} \right) \rangle , \end{aligned} \quad (42)$$

and,

$$\begin{aligned}
f_q(q) &= \frac{1}{a} f(e), \quad q \in \langle 0, a \rangle, \\
f(e) &= f[g^{-1}(e)] \frac{1}{|\cos \chi + X_{e2}|}, \\
X_{e2} &= \frac{(2e-1) \cos \chi \sin \chi + 2\sqrt{e(1-e)} \sin^2 \chi}{\sqrt{1 + [1 + 8e(e-1)] |\sin \chi| \sin \chi - (2e-1)^2 - 4(2e-1)\sqrt{e(1-e)} |\sin \chi| \cos \chi}}, \\
e_{in} &= g^{-1}(e) = + \sqrt{e(1-e)} |\sin \chi| + \frac{1}{2} [1 + (2e-1) \cos \chi], \\
e &= 1 - \frac{q}{a}, \\
\chi &= \frac{2\pi}{P} t, \\
e_{in} &\in \langle \sin^2 \left(\frac{\pi t}{P} \right), 1 \rangle.
\end{aligned} \tag{43}$$

The probability $P(q < q_L)$ that a perihelion distance q is less than a given value q_L can be calculated from

$$\begin{aligned}
P(q < q_L) &= \int_0^{q_L} f_q(q') dq', \\
P(q < q_L) &= F_q(q_L).
\end{aligned} \tag{44}$$

where Eqs. (42)-(43) are to be used.

6.1.1. Uniform distribution

Let us consider, as an example, a uniform distribution of eccentricities. The density and distribution functions of perihelion distance are, on the basis of Eqs. (29), (41) and Eqs. (44),

$$\begin{aligned}
f_q(q_{in}) &= \frac{1}{a}, \\
F_q(q_{in}) &= \int_0^{q_{in}} f_q(q'_{in}) dq'_{in} = q_{in}/a, \\
q_{in} &\in \langle 0, a \rangle.
\end{aligned} \tag{45}$$

The distribution function $F(q_{in})$ fulfills the condition $F_q(a) = 1$.

Using Eqs. (42)-(43), we obtain

$$\begin{aligned}
f(e) &= \frac{1}{a} \frac{1}{|\cos \chi + X_{e1}|}, \\
X_{e1} &= \frac{(2e-1) \cos \chi \sin \chi - 2\sqrt{e(1-e)} |\sin \chi| \sin \chi}{\sqrt{1 + [1 + 8e(e-1)] \sin^2 \chi - (2e-1)^2 + 4(2e-1)\sqrt{e(1-e)} |\sin \chi| \cos \chi}}, \\
e &= 1 - \frac{q}{a}, \\
\chi &= \frac{2\pi}{P} t, \\
e_{in} &\in \langle 0, \sin^2 \left(\frac{\pi t}{P} \right) \rangle,
\end{aligned} \tag{46}$$

and,

$$f(e) = \frac{1}{a} \frac{1}{|\cos \chi + X_{e2}|},$$

$$\begin{aligned}
X_{e2} &= \frac{(2e-1) \cos \chi \sin \chi + 2\sqrt{e(1-e)} \sin^2 \chi}{\sqrt{1 + [1 + 8e(e-1)] |\sin \chi| \sin \chi - (2e-1)^2 - 4(2e-1)\sqrt{e(1-e)} |\sin \chi| \cos \chi}}, \\
e &= 1 - \frac{q}{a}, \\
\chi &= \frac{2\pi}{P} t, \\
e_{in} &\in \langle \sin^2 \left(\frac{\pi t}{P} \right), 1 \rangle.
\end{aligned} \tag{47}$$

As an illustration we take $t = P/2$. Eqs. (46)-(47) yield $f_q(q) = 1/a$, and, the distribution function is $F_q(q) = q/a$:

$$\begin{aligned}
f_q(q) &= \frac{1}{a}, \quad t = 0, \\
F_q(q) &= \frac{q}{a}, \quad t = 0, \\
f_q(q) &= \frac{1}{a}, \quad t = \frac{P}{2}, \\
F_q(q) &= \frac{q}{a}, \quad t = \frac{P}{2}.
\end{aligned} \tag{48}$$

Eqs. (44) may be used.

6.1.2. Distribution function $F(e_{in}) = e_{in}^2$

We will consider, as an another example, $F(e_{in}) = e_{in}^2$ (see Sec. 5.1.2). The corresponding density and distribution functions of perihelion distance are, on the basis of Eqs. (33), (41) and Eqs.(44),

$$\begin{aligned}
f_q(q_{in}) &= 2 \frac{1}{a} \left(1 - \frac{q_{in}}{a} \right), \\
F_q(q_{in}) &= \int_0^{q_{in}} f_q(q'_{in}) dq'_{in} = \frac{q_{in}}{a} \left(2 - \frac{q_{in}}{a} \right), \\
q_{in} &\in \langle 0, a \rangle.
\end{aligned} \tag{49}$$

Using Eqs. (42)-(43), we obtain

$$\begin{aligned}
f_q(q) &= \frac{1}{a} f(e), \quad q \in \langle 0, a \rangle, \\
f(e) &= \frac{1 + (2e-1) \cos \chi - 2\sqrt{e(1-e)} |\sin \chi|}{|\cos \chi + X_{e1}|}, \\
X_{e1} &= \frac{(2e-1) \cos \chi \sin \chi - 2\sqrt{e(1-e)} |\sin \chi| \sin \chi}{\sqrt{1 + [1 + 8e(e-1)] \sin^2 \chi - (2e-1)^2 + 4(2e-1)\sqrt{e(1-e)} |\sin \chi| \cos \chi}}, \\
e &= 1 - \frac{q}{a}, \\
\chi &= \frac{2\pi}{P} t, \\
e_{in} &\in \langle 0, \sin^2 \left(\frac{\pi t}{P} \right) \rangle,
\end{aligned} \tag{50}$$

and,

$$\begin{aligned}
f_q(q) &= \frac{1}{a} f(e), \quad q \in \langle 0, a \rangle, \\
f(e) &= \frac{1 + (2e-1) \cos \chi + 2\sqrt{e(1-e)} |\sin \chi|}{|\cos \chi + X_{e2}|},
\end{aligned}$$

$$\begin{aligned}
X_{e2} &= \frac{(2e-1) \cos \chi \sin \chi + 2\sqrt{e(1-e)} \sin^2 \chi}{\sqrt{1 + [1 + 8e(e-1)] |\sin \chi| \sin \chi - (2e-1)^2 - 4(2e-1)\sqrt{e(1-e)} |\sin \chi| \cos \chi}}, \\
e &= 1 - \frac{q}{a}, \\
\chi &= \frac{2\pi}{P} t, \\
e_{in} &\in \langle \sin^2 \left(\frac{\pi t}{P} \right), 1 \rangle.
\end{aligned} \tag{51}$$

As an illustration we take $t = P/2$. Eqs. (50)-(51) yield $f_q(q) = 2 q/a^2$, and, the distribution function is $F_q(q) = (q/a)^2$:

$$\begin{aligned}
f_q(q) &= 2 \frac{1}{a} \left(1 - \frac{q}{a} \right), \quad t = 0, \\
F_q(q) &= \frac{q}{a} \left(2 - \frac{q}{a} \right), \quad t = 0, \\
f_q(q) &= 2 \frac{1}{a} \frac{q}{a}, \quad t = \frac{P}{2}, \\
F_q(q) &= \left(\frac{q}{a} \right)^2, \quad t = \frac{P}{2}, \\
q &\in \langle 0, a \rangle.
\end{aligned} \tag{52}$$

The situation represented by Eqs. (52) is illustrated in Fig. 7.

6.2. $P(q < q_L)$ for a random time

Orbital evolution of perihelion distance is given by the evolution of eccentricity, since the relation between the semi-major axis a and eccentricity e is $q = a(1 - e)$, and a is a constant in secular evolution due to the tidal effect of the Galaxy. We have, on the basis of Eqs. (19),

$$\begin{aligned}
q(t) &= \frac{a}{2} \left\{ 1 + \sin \left(\frac{2\pi}{P} t - \frac{\pi}{2} \delta_{in} \right) \right\}, \\
\delta_{in} &\in \langle -1, +1 \rangle.
\end{aligned} \tag{53}$$

The probability $P(q < q_L)$ that a value q is smaller than a value q_L , in the sense of Sec. 5.2, is

$$P(q < q_L) = \frac{1}{2} - \frac{1}{\pi} \arcsin \left(1 - 2 \frac{q_L}{a} \right). \tag{54}$$

If $q_L/a \ll 1$, then Eq. (54) reduces to

$$P(q < q_L) = \frac{2}{\pi} \sqrt{\frac{q_L}{a}}, \quad q_L/a \ll 1. \tag{55}$$

If one uses the form $q = a |1 - 2 |t - t_{in}|(\text{mod } P)/P|$ instead of Eq. (53), then $P(q < q_L) = q_L/a$. Eqs. (54)-(55) hold for the case when gravity of the Sun and galactic tide are considered.

6.3. Distribution of perihelion distances – galactic tides and results of numerical calculations

Fig. 8 illustrates distribution of perihelion distances, histogram and cumulative number of comets $N(< q)$ as a function of a cometary perihelion distance q . The results presented in Fig. 8 correspond to the gravity of the Sun and the effect of galactic tide, only. Numerical integrations of equation of motion for 4.5×10^9 years for semi-major axis $a_{in} = 5 \times 10^4$ AU, inclination with respect to the galactic equatorial plane $i_{in} = 90$ degrees and various orientations of the initially almost circular orbits (rotation angles – longitudes of the ascending node – 0, 45, 90, ..., 270, 315 degrees) were performed.

The histogram for the zone $q < 30$ (40) AU suggests that the q -distribution corresponds to the uniform distribution and it is consistent with the observational data for the group of “new” comets presented by Fernández and Gallardo (1999, Fig. 1).

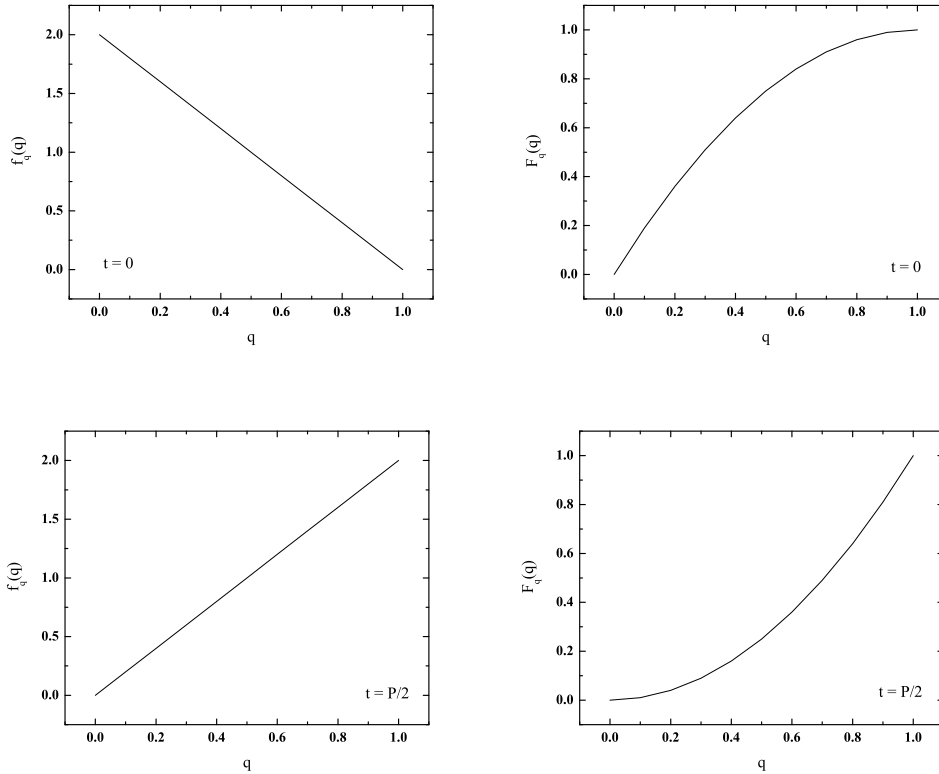


Fig. 7. Density $f_q(q)$ and distribution $F_q(q)$ functions of perihelion distance for two instants: $t = 0$ and $t = P/2$, where P is the oscillation period of eccentricities (perihelion and aphelion distances, angular orbital elements). Galactic tide and gravity of the Sun play role. Semi-major axis is normed to 1, for simplicity.

On the basis of the histogram in Fig. 8 one could come to the conclusion that the distribution function of perihelia is given by Eq. (49) and the situation corresponds to the idea of Fernández and Gallardo (1999), Hills (1981) and Jeans (1919), as it was mentioned in Sec. 6.1.2. If the idea is physically correct, one should await that the cumulative number of comets $N(< q)$ is given by the formula represented by Eq. (49). The least-square method fit to the data yields

$$\begin{aligned}
 N(< q) &= A q + B q^2, \quad q \ll a, \\
 A &= (1.08 \pm 0.03) \text{ AU}^{-1}, \\
 B &= - (4.9 \pm 0.3) \times 10^{-3} \text{ AU}^{-2}.
 \end{aligned} \tag{56}$$

The comets with $a = 5 \times 10^4$ AU are used. Eq. (49) yields that $A = 2 / a$ and $B = - 1 / a^2$ and their ratio is $|B|/A = 1 / (2 a) = 1 \times 10^{-5} \text{ AU}^{-1}$. Eq. (56) yields $|B|/A = 4.54 \times 10^{-3} \text{ AU}^{-1}$, i.e., 454-times greater than the value corresponding to the idea of Jeans (1919), Hills (1981) and others.

On the basis of Sec. 6.2 we have tried also the fit of the form $N(< q) = C q^\gamma$. The least-square method yields

$$\begin{aligned}
 N(< q) &= C_\gamma q^\gamma, \quad q \ll a, \\
 C_\gamma &= (3.055 \pm 0.335) \text{ AU}^{-\gamma}, \\
 \gamma &= 0.657 \pm 0.026.
 \end{aligned} \tag{57}$$

The value of the exponent γ lies between the values 1/2 and 1 discussed in Sec. 6.2. The result suggests that γ equals 2/3. If we use the least-square fit of the form $N(< q) = C q^{2/3}$, we obtain

$$N(< q) = C q^{2/3}, \quad q \ll a,$$

$$C = (2.929 \pm 0.032) \text{ AU}^{-3/2} . \quad (58)$$

The error of C is 1%.

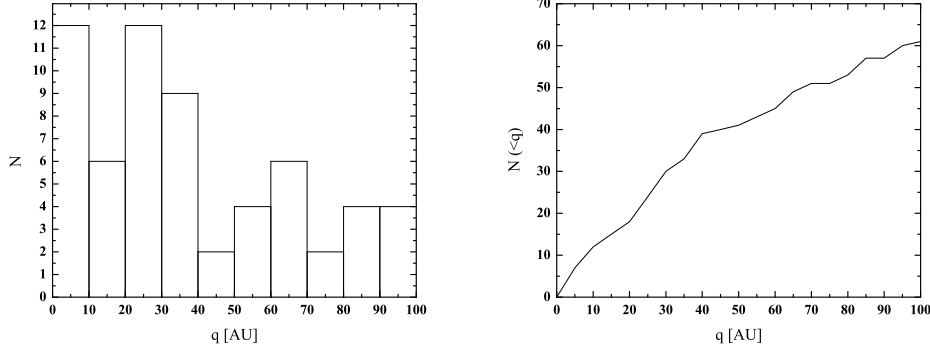


Fig. 8. Histogram and number $N(< q)$ of comets with perihelia smaller than a value q of the perihelion distance. Only cases for the inner part of the Solar System are depicted, $q < 100$ AU.

The idea of Fernández and Gallardo (1999), Hills (1981) and Jeans (1919) (and others) is based on the density function $f(e) = 2 e$ or $f_q(q) = (2/a)(1 - q/a)$. However, also other functions can produce uniform distribution in perihelion distances for small q , e.g., $f(e) = (k+1)e^k$, $f_q(q) = [(1+k)/a](1 - q/a)^k$, $F_q(q) = 1 - (1 - q/a)^{k+1}$ ($k > -1$); $F_q(q) = (k+1)q/a$ for small q . Moreover, the distribution treated by Jeans (1919) yields not only a density function for eccentricity, but also a density function for semi-major axis. The density function for semi-major axis is, according to Jeans (1919), proportional to \sqrt{a} . This is not consistent with the idea that the distribution in semi-major axis is a^α , where $\alpha \in (-4, -2)$ (Fernández and Gallardo 1999). Thus Eq. (58) may be more physical than Eq. (56).

6.4. Distribution functions $F_{a, e}(a, e)$, $F_{a, q}(a, q)$, $F_q(q)$, $F_a(a)$

We want to find distribution functions $F_{a, e}(a, e)$, $F_{a, q}(a, q)$ and $F_q(q)$, where a , e and q are the semi-major axis, eccentricity and perihelion distance.

6.4.1. Distribution function $F_{a, e}(a, e)$

If the density function $f_{a, e}(a, e)$ can be written as the product $f_a(a) f(e)$, then

$$F_{a, e}(a, e) = \int_{a_{min}}^a f_a(a') da' \int_0^e f(e') de' ,$$

$$a \in \langle a_{min}, a_{max} \rangle ,$$

$$e \in \langle 0, 1 \rangle . \quad (59)$$

Let ($\alpha \neq -1$)

$$f_a(a) = (\alpha + 1) (a_{max}^{\alpha+1} - a_{min}^{\alpha+1})^{-1} a^\alpha ,$$

$$f(e) = (k + 1) e^k , \quad k > 0 ,$$

$$a \in \langle a_{min}, a_{max} \rangle ,$$

$$e \in \langle 0, 1 \rangle . \quad (60)$$

Eqs. (59)-(60) yield

$$F_{a, e}(a, e) = \frac{a^{\alpha+1} - a_{min}^{\alpha+1}}{a_{max}^{\alpha+1} - a_{min}^{\alpha+1}} e^{k+1} ,$$

$$\begin{aligned} a &\in \langle a_{min}, a_{max} \rangle , \\ e &\in \langle 0, 1 \rangle . \end{aligned} \tag{61}$$

The case $\alpha = -1$ would yield

$$\begin{aligned} f_a(a) &= (\ln a_{max} - \ln a_{min})^{-1} a^{-1} , \\ F_{a, e}(a, e) &= \frac{\ln a - \ln a_{min}}{\ln a_{max} - \ln a_{min}} e^{k+1} , \\ a &\in \langle a_{min}, a_{max} \rangle , \\ e &\in \langle 0, 1 \rangle , \end{aligned} \tag{62}$$

instead of Eqs. (61).

6.4.2. Distribution function $F_{a, q}(a, q)$

We have to use $e = 1 - q / a$ in Sec. 6.4.1.

In general, we have

$$\begin{aligned} F_{a, q}(a, q) &= \int_{a_{min}}^a \int_{1-q/a_1}^1 f_{a, e}(a_1, e) de da_1 , \\ a &\in \langle a_{min}, a_{max} \rangle , \\ q &\in \langle 0, a_{min} \rangle , \\ F_{a, q}(a, q) &= \int_{a_{min}}^q \int_0^1 f_{a, e}(a_1, e) de da_1 \\ &\quad + \int_q^a \int_{1-q/a_1}^1 f_{a, e}(a_1, e) de da_1 , \\ a &\in \langle a_{min}, a_{max} \rangle , \\ q &\in \langle a_{min}, a \rangle . \end{aligned} \tag{63}$$

If we consider the conventional approach $k = 1$ (e.g., Hills 1981, Fernández and Gallardo 1999), then Eqs. (63) yield

$$\begin{aligned} F_{a, q}(a, q) &= \frac{\alpha + 1}{a_{max}^{\alpha+1} - a_{min}^{\alpha+1}} \left\{ \frac{2}{\alpha} q (a^\alpha - a_{min}^\alpha) - \frac{1}{\alpha - 1} q^2 (a^{\alpha-1} - a_{min}^{\alpha-1}) \right\} , \\ a &\in \langle a_{min}, a_{max} \rangle , \\ q &\in \langle 0, a_{min} \rangle , \\ F_{a, q}(a, q) &= \frac{q^{\alpha+1} - a_{min}^{\alpha+1}}{a_{max}^{\alpha+1} - a_{min}^{\alpha+1}} \\ &\quad + \frac{\alpha + 1}{a_{max}^{\alpha+1} - a_{min}^{\alpha+1}} \left\{ \frac{2}{\alpha} q (a^\alpha - q^\alpha) - \frac{1}{\alpha - 1} q^2 (a^{\alpha-1} - q^{\alpha-1}) \right\} , \\ a &\in \langle a_{min}, a_{max} \rangle , \\ q &\in \langle a_{min}, a \rangle . \end{aligned} \tag{64}$$

If k is more general, not only the special case $k = 1$, then Eqs. (63) yield ($\alpha \neq -1$)

$$\begin{aligned} F_{a, q}(a, q) &= \frac{\alpha + 1}{a_{max}^{\alpha+1} - a_{min}^{\alpha+1}} \int_{a_{min}}^a a_1^\alpha \left\{ 1 - \left(1 - \frac{q}{a_1} \right)^{k+1} \right\} da_1 = \\ &= \frac{\alpha + 1}{a_{max}^{\alpha+1} - a_{min}^{\alpha+1}} \sum_{l=1}^{k+1} \binom{k+1}{l} \frac{(-1)^{l+1}}{\alpha + 1 - l} q^l (a^{\alpha+1-l} - a_{min}^{\alpha+1-l}) , \\ q &\in \langle 0, a_{min} \rangle , \\ a &\in \langle a_{min}, a_{max} \rangle , \end{aligned}$$

$$\begin{aligned}
F_{a, q}(a, q) &= \frac{q^{\alpha+1} - a_{min}^{\alpha+1}}{a_{max}^{\alpha+1} - a_{min}^{\alpha+1}} \\
&+ \frac{\alpha + 1}{a_{max}^{\alpha+1} - a_{min}^{\alpha+1}} \int_q^a a_1^\alpha \left\{ 1 - \left(1 - \frac{q}{a_1} \right)^{k+1} \right\} da_1 = \\
&= \frac{q^{\alpha+1} - a_{min}^{\alpha+1}}{a_{max}^{\alpha+1} - a_{min}^{\alpha+1}} \\
&+ \frac{\alpha + 1}{a_{max}^{\alpha+1} - a_{min}^{\alpha+1}} \sum_{l=1}^{k+1} \binom{k+1}{l} \frac{(-1)^{l+1}}{\alpha + 1 - l} q^l (a^{\alpha+1-l} - q^{\alpha+1-l}), \\
q &\in \langle a_{min}, a \rangle, \\
a &\in \langle a_{min}, a_{max} \rangle.
\end{aligned} \tag{65}$$

Of course, k may not be an integer number.

The conventional statements on the Oort cloud are: $\alpha = -3/2$ or $\alpha \in (-4, -2)$ and $f(e) = 2e$ (e.g., Duncan et al. 1987, Bailey 1983, Fernández and Ip 1987, Fernández 1992, Fernández and Gallardo 1999). We have obtained some results on the values of α and a_{min} already in Sec. 2, see the last paragraph of Sec. 2. Also results from Secs. 9 and 10 will be helpful.

6.4.3. Distribution function $F_q(q)$

We have found that $F_{a, q}(a, q)$ is represented by Eqs. (64) if $f(e) = 2e$. If we are interested in $F_q(q)$, then we have to consider $a \in \langle a_{min}, a_{max} \rangle$. We obtain $F_q(q) = F_{a, q}(a_{max}, q)$, or

$$\begin{aligned}
F_q(q) &= \frac{\alpha + 1}{a_{max}^{\alpha+1} - a_{min}^{\alpha+1}} \left\{ \frac{2}{\alpha} q (a_{max}^\alpha - a_{min}^\alpha) - \frac{1}{\alpha - 1} q^2 (a_{max}^{\alpha-1} - a_{min}^{\alpha-1}) \right\}, \\
q &\in \langle 0, a_{min} \rangle, \\
F_q(q) &= \frac{q^{\alpha+1} - a_{min}^{\alpha+1}}{a_{max}^{\alpha+1} - a_{min}^{\alpha+1}} \\
&+ \frac{\alpha + 1}{a_{max}^{\alpha+1} - a_{min}^{\alpha+1}} \left\{ \frac{2}{\alpha} q (a_{max}^\alpha - q^\alpha) - \frac{1}{\alpha - 1} q^2 (a_{max}^{\alpha-1} - q^{\alpha-1}) \right\}, \\
q &\in \langle a_{min}, a_{max} \rangle.
\end{aligned} \tag{66}$$

Eq. (66) improves the result of, e.g., Hills (1981), Fernández and Gallardo (1999).

The case of arbitrary k , given by Eqs. (65), leads to

$$\begin{aligned}
F_q(q) &= \frac{\alpha + 1}{a_{max}^{\alpha+1} - a_{min}^{\alpha+1}} \int_{a_{min}}^{a_{max}} a_1^\alpha \left\{ 1 - \left(1 - \frac{q}{a_1} \right)^{k+1} \right\} da_1 = \\
&= \frac{\alpha + 1}{a_{max}^{\alpha+1} - a_{min}^{\alpha+1}} \sum_{l=1}^{k+1} \binom{k+1}{l} \frac{(-1)^{l+1}}{\alpha + 1 - l} q^l (a_{max}^{\alpha+1-l} - a_{min}^{\alpha+1-l}), \\
q &\in \langle 0, a_{min} \rangle, \\
F_q(q) &= \frac{q^{\alpha+1} - a_{min}^{\alpha+1}}{a_{max}^{\alpha+1} - a_{min}^{\alpha+1}} \\
&+ \frac{\alpha + 1}{a_{max}^{\alpha+1} - a_{min}^{\alpha+1}} \int_q^{a_{max}} a_1^\alpha \left\{ 1 - \left(1 - \frac{q}{a_1} \right)^{k+1} \right\} da_1 = \\
&= \frac{q^{\alpha+1} - a_{min}^{\alpha+1}}{a_{max}^{\alpha+1} - a_{min}^{\alpha+1}} \\
&+ \frac{\alpha + 1}{a_{max}^{\alpha+1} - a_{min}^{\alpha+1}} \sum_{l=1}^{k+1} \binom{k+1}{l} \frac{(-1)^{l+1}}{\alpha + 1 - l} q^l (a_{max}^{\alpha+1-l} - q^{\alpha+1-l}), \\
q &\in \langle a_{min}, a_{max} \rangle.
\end{aligned} \tag{67}$$

As a consequence, $F_q(q) \propto q^1$, for small q , holds for arbitrary k , not only for $k = 1$ or k integer. Thus, the result of observations (inner part of the Solar System) yielding $F_q(q) \propto q^1$ cannot be used as an argument for $f(e) = 2 e$.

6.4.4. Distribution function $F_a(a)$

The distribution and density functions $F_a(a)$ and $f_a(a)$ are

$$F_a(a) = \frac{a^{\alpha+1} - a_{min}^{\alpha+1}}{a_{max}^{\alpha+1} - a_{min}^{\alpha+1}},$$

$$f_a(a) = (\alpha + 1) \frac{a^\alpha}{a_{max}^{\alpha+1} - a_{min}^{\alpha+1}},$$

$$a \in \langle a_{min}, a_{max} \rangle, \quad (68)$$

if Eqs. (61) and relation $F_a(a) = \int_0^a f_a(a') da'$ are used.

7. Minimal perihelion distances and inclinations for comets with “moderate” initial inclinations

In order to determine some basic properties of secular orbital evolution of a comet under the action of the galactic tide we numerically solved the system of Eqs. (13)-(17) in Pástor et al. (2009). We consider two values of the semi-major axis, 10 000 AU and 20 000 AU, as examples. We do not consider greater values of the semi-major axis since the analytical approach to the secular evolution of orbital elements does not yield results equivalent to the results obtained by detailed solution of equation of motion (Pástor et al. 2009).

Table 3 presents numerical solutions q_{min} and inclinations i_{min} corresponding to the minimal perihelion distances q_{min} . Also oscillation periods P are given in Table 3. By the term “inclination” we mean the inclination with respect to the galactic equatorial plane. Table 3 also shows initial conditions of the numerical integrations. Initial argument of perihelion is used only from interval $\omega_{in} \in \langle 0, 180^\circ \rangle$. This is sufficient since orbital evolution for $\omega_{in} = \omega + 180^\circ$ is identical to the evolution for $\omega_{in} = \omega$ if the values of other initial orbital elements are fixed (Pástor et al. 2009). We found that evolutions of eccentricity, argument of perihelion and inclination are not very sensitive to initial value of the ascending node for the initial inclination $i_{in} \lesssim 80^\circ$ (under the assumption that the values of other initial orbital elements are fixed). Graphical evolutions of the ascending node for various values of Ω_{in} are approximately parallel, in this case (the parallelism does not hold for the case $i_{in} \approx 90^\circ$). This is the reason why the initial ascending node equals to zero for all numerical integrations in Table 3. Table 3 also shows that the minimal perihelion distance is a decreasing function of i_{in} , if the values of other initial orbital elements are fixed. In reality, comets with initial inclinations close to 90° can get into the interior region of the Solar System due to the galactic tide.

Fig. 9 depicts inclination i_{min} at minimal perihelion distance as a function of minimal perihelion distance q_{min} . The values are taken from Table 3. i_{min} is an increasing function of q_{min} for a given a_{in} and i_{in} . Comparison of the values of q_{min} at $a_{in} = 10\,000$ AU and $20\,000$ AU, for a fixed ω_{in} and i_{in} , yields

$$\frac{q_{min\ 1}}{q_{min\ 2}} \approx \frac{a_{in\ 1}}{a_{in\ 2}}. \quad (69)$$

If a_{in} and i_{in} are fixed, then the values $\omega_{in} = \omega$ and $\omega_{in} = 180^\circ - \omega$ yield approximately equal values of q_{min} and i_{min} (see also Table 3). This is the reason why we can see only five distinct points, not eight, in Fig. 9. This property is not related only to the values of q_{min} and i_{min} : the complete orbital evolutions of the comets are very similar for $\omega_{in} = \omega$ and $\omega_{in} = 180^\circ - \omega$. This property divides the interval $\omega_{in} \in \langle 0, 180^\circ \rangle$ into two parts with different behavior. If we consider only the values $\omega_{in} \in \langle 0, 90^\circ \rangle$, then q_{min} and i_{min} are increasing functions of ω_{in} , if a_{in} and i_{in} are fixed. If $\omega_{in} \in \langle 90^\circ, 180^\circ \rangle$, then q_{min} and i_{min} are decreasing functions of ω_{in} . An explanation of this property is probably in the antisymmetry of the secular time derivatives after transformations $\omega \rightarrow \pi - \omega$, $\Omega \rightarrow \pi - \Omega$ (Pástor et al. 2009). Since the orbital evolution is not very sensitive to the initial value of the ascending node, we obtain similar orbital evolution for $\omega_{in} = 180^\circ - \omega$ as for $\omega_{in} = \omega$.

j	a_{in}	e_{in}	ω_{in}	Ω_{in}	i_{in}	t_{int}	q_{min}	i_{min}	P
[-]	[AU]	[-]	[°]	[°]	[°]	[10^{10} years]	[AU]	[°]	[10^9 years]
1	10 000	0.4	0	0	30	2	4449	18.04	4.3
2	10 000	0.4	22.5	0	30	2	4565	19.50	4.6
3	10 000	0.4	45	0	30	2	4916	23.10	5.8
4	10 000	0.4	67.5	0	30	2	5496	27.35	9.7
5	10 000	0.4	90	0	30	2	5998	30.02	7.0
6	10 000	0.4	112.5	0	30	2	5497	27.36	9.7
7	10 000	0.4	135	0	30	2	4915	23.09	5.8
8	10 000	0.4	157.5	0	30	2	4565	19.51	4.6
9	10 000	0.4	0	0	60	2	1315	23.98	3.9
10	10 000	0.4	22.5	0	60	2	1351	25.41	4.7
11	10 000	0.4	45	0	60	2	1465	29.44	4.0
12	10 000	0.4	67.5	0	60	2	1614	33.39	3.1
13	10 000	0.4	90	0	60	2	1691	35.10	2.9
14	10 000	0.4	112.5	0	60	2	1613	33.41	3.1
15	10 000	0.4	135	0	60	2	1466	29.46	4.0
16	10 000	0.4	157.5	0	60	2	1348	25.37	4.7
17	20 000	0.4	0	0	30	2	8722	17.99	1.5
18	20 000	0.4	22.5	0	30	2	8973	19.40	1.6
19	20 000	0.4	45	0	30	2	9700	23.03	2.0
20	20 000	0.4	67.5	0	30	2	10915	27.30	3.4
21	20 000	0.4	90	0	30	2	11990	30.05	2.5
22	20 000	0.4	112.5	0	30	2	10921	27.28	3.4
23	20 000	0.4	135	0	30	2	9698	23.01	2.0
24	20 000	0.4	157.5	0	30	2	8968	19.40	1.6
25	20 000	0.4	0	0	60	2	2485	23.61	1.4
26	20 000	0.4	22.5	0	60	2	2572	25.32	1.6
27	20 000	0.4	45	0	60	2	2805	29.34	1.4
28	20 000	0.4	67.5	0	60	2	3116	33.36	1.1
29	20 000	0.4	90	0	60	2	3268	35.04	1.0
30	20 000	0.4	112.5	0	60	2	3109	33.31	1.1
31	20 000	0.4	135	0	60	2	2804	29.35	1.4
32	20 000	0.4	157.5	0	60	2	2573	25.33	1.6

Table 3. Inclinations i_{min} corresponding to minimal perihelion distances q_{min} and oscillation periods P as a result of numerical integration of the system of differential equations for secular evolution of orbital elements. Time of integration is $t_{int} 2 \times 10^{10}$ years. The initial semi-major axis a_{in} , eccentricity e_{in} , argument of perihelion ω_{in} , longitude of the ascending node Ω_{in} and inclination i_{in} are shown.

8. Distribution in the ecliptical inclination

If we want to consider cometary orbital elements for the inner part of the Solar System, then we have to consider initial inclinations with respect to the galactic equatorial plane close to 90 degrees (see also Sec. 7). Gravity of the Sun and Galaxy will be considered.

We used numerical solution of the system of equations for secular evolution of orbital elements given by Eqs. (13)-(17) in Pástor et al. (2009). We used the equations to measure minimal perihelion distance q_{min} of a comet at the first three returns of the comet to the inner part of the Solar System. At the time when the minimal perihelion distance occurred we measured also the inclination i_{min} and the longitude of the ascending node Ω_{min} . The results are shown in Table 4. Initial conditions of numerical integrations are also shown. Numerical integrations with equal values of initial semi-major axes, eccentricities and arguments of perihelion have equal oscillation period. The oscillation period for all numerical integrations in Table 4 is $P \approx 1.3 \times 10^9$ years. Change of the longitude of the ascending node Ω of the comet with initial inclination $i_{in} \approx 90^\circ$ during the return of the comet to the inner part of the Solar System is always $\approx \pm\pi$. The last column shows two "stable" values fulfilling the fact that Ω lies between the values at perihelion. If the first value is smaller/greater than the second one, then Ω increases/decreases from the first value to the second one.

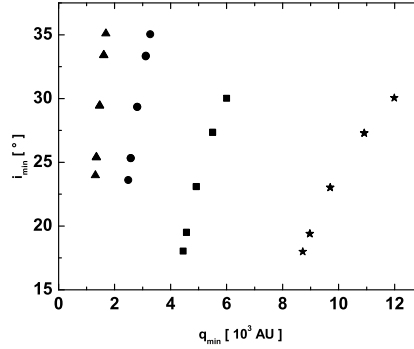


Fig. 9. Inclination to galactic equatorial plane at minimal perihelion distance q_{min} . Square is used for $a_{in} = 10\,000$ AU and $i_{in} = 30^\circ$, triangle for $a_{in} = 10\,000$ AU and $i_{in} = 60^\circ$, star for $a_{in} = 20\,000$ AU and $i_{in} = 30^\circ$ and circle for $a_{in} = 20\,000$ AU and $i_{in} = 60^\circ$. The greater i_{in} , the smaller q_{min} and the greater i_{min} , for a given a_{in} .

We are interested in an inclination i of the cometary orbital plane with respect to a reference plane. The reference plane is defined by the inclination i_0 and the longitude of the ascending node Ω_0 with respect to the galactic equatorial plane (and a given reference direction). If the galactic inclination of the comet at its perihelion is i_{min} (galactic longitude of the ascending node Ω_{min}), then the inclination i at perihelion position can be calculated from the following equation:

$$\cos i = \cos i_0 \cos i_{min} + \sin i_0 \sin i_{min} \cos(\Omega_0 - \Omega_{min}) . \quad (70)$$

Table 4 shows that the values of inclination with respect to the galactic equator (galactic inclination) are always close to 25° or 155° . The number of comets with galactic inclination close to 25° is approximately equal to the number of comets with the inclination close to 155° . The values of Ω_{min} are practically random (see also Table 4). These facts yield for a large sample of comets

$$\begin{aligned} h_H(i) &= \frac{1}{2} \sin i , \\ H(i) &= \frac{1}{2} (1 - \cos i) , \\ \langle \cos i \rangle &= 0 , \\ \langle i \rangle &= \frac{\pi}{2} . \end{aligned} \quad (71)$$

The results state that the density and distribution functions correspond to isotropic distribution, the average value of $\cos i$ equals zero and the average value of i is $\pi / 2$. The results are consistent with Eqs. (6).

The results presented in Eqs. (71) hold for inclinations with respect to any reference plane $i_0 \neq 0$, also for the ecliptic plane. The distribution of galactic inclinations for comets in the inner part of the Solar System is not isotropic, if only gravity of the Sun and Galaxy are considered: $i(galactic) \approx 25^\circ$ or 155° .

9. Gravity of the Galaxy, Sun and Jupiter

This section presents results obtained when also gravity of the planet Jupiter is included.

9.1. Evolution of orbital elements

Evolution of semi-major axis and eccentricity is depicted in Fig. 10. The action of the Sun and Galaxy produces constant semi-major axis of a comet in the Oort cloud, as for secular orbital evolution. The

j	a_{in}	e_{in}	ω_{in}	Ω_{in}	i_{in}	q_{min}	i_{min}	Ω_{min}	interval
[-]	[AU]	[-]	[°]	[°]	[°]	[AU]	[°]	[°]	[°]
1	20 000	0.4	0	0	90	1.38	151.31	124.04	(0,180)
2	20 000	0.4	0	0	90	0.82	24.56	97.06	(180,0)
3	20 000	0.4	0	0	90	2.07	151.69	59.15	(0,180)
4	20 000	0.4	0	45	90	2.17	24.80	-34.21	(45,-135)
5	20 000	0.4	0	45	90	0.39	153.57	-68.24	(-135,45)
6	20 000	0.4	0	45	90	0.11	155.36	128.71	(45,225)
7	20 000	0.4	0	90	90	1.96	25.70	-19.22	(90,-90)
8	20 000	0.4	0	90	90	0.66	155.40	5.56	(-90,90)
9	20 000	0.4	0	90	90	3.12	25.16	14.47	(90,-90)
10	20 000	0.4	0	135	90	0.51	152.69	196.98	(135,315)
11	20 000	0.4	0	135	90	0.03	155.43	411.06	(315,495)
12	20 000	0.4	0	135	90	1.99	25.25	389.91	(495,315)
13	20 000	0.4	0	180	90	1.20	153.99	291.56	(180,360)
14	20 000	0.4	0	180	90	0.81	24.54	264.51	(360,180)
15	20 000	0.4	0	180	90	1.72	150.34	234.41	(180,360)
16	20 000	0.4	0	225	90	2.29	24.44	132.57	(225,45)
17	20 000	0.4	0	225	90	0.45	154.20	115.59	(45,225)
18	20 000	0.4	0	225	90	0.31	153.50	339.85	(225,405)
19	20 000	0.4	0	270	90	1.67	27.66	150.12	(270,90)
20	20 000	0.4	0	270	90	0.90	154.07	200.37	(90,270)
21	20 000	0.4	0	270	90	2.79	26.85	206.01	(290,90)
22	20 000	0.4	0	315	90	0.87	149.92	366.91	(315,495)
23	20 000	0.4	0	315	90	0.11	154.00	606.52	(495,675)
24	20 000	0.4	0	315	90	2.05	25.70	566.40	(675,495)

Table 4. Minimal perihelion distances q_{min} during the first three returns of a comet to the inner part of the Solar System. Inclinations i_{min} and longitudes of the ascending nodes Ω_{min} corresponding to minimal perihelion distances are given. Initial semi-major axis a_{in} , eccentricity e_{in} , argument of perihelion ω_{in} , longitude of the ascending node Ω_{in} and inclination i_{in} are shown. The longitude of the ascending node rapidly changes around Ω_{in} within the interval presented in the last column.

presence of Jupiter may cause sudden changes in semi-major axis. Moreover, the planet caused that the period of oscillations in eccentricity (perihelion and aphelion distances, inclination, ...) decreased to almost one half of the period found without the action of the planet.

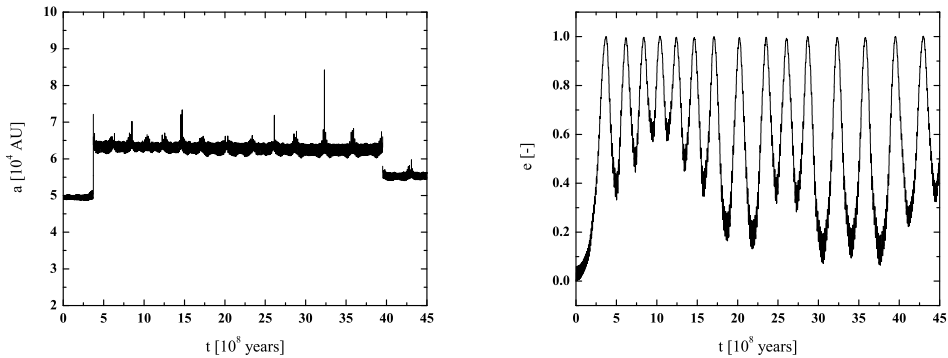


Fig. 10. Evolution of semi-major axis and eccentricity for a comet under the gravitational influence of the Sun, Galaxy and Jupiter.

9.2. Distribution in perihelion distance

As it is presented in the previous subsection (see Fig. 10), the presence of Jupiter may cause more frequent returns of a comet to the inner part of the Solar System than it is in the case when the planet is ignored. Moreover, our calculations confirmed the importance of the planet also in another type of computational experiment. We considered the same initial conditions (orbital elements – semi-major axis 5×10^4 AU, inclination with respect to the galactic equatorial plane 90 degrees, eccentricity close to zero, ...) for the two cases, one without Jupiter and one with the action of Jupiter. We gathered long-period comets with perihelion distance q less than 100 AU (two groups of comets do not belong to the set of comets: i) comets with $q < 0.01$ AU, and ii) comets ejected from the Solar System due to the close approach to Jupiter). While the ignorance of Jupiter yielded that 5.0% of the comets exhibited $q < 5$ AU, the action of Jupiter, Sun and Galaxy yielded that 28.6% of the comets exhibited $q < 5$ AU. The corresponding percentages for $q < 10$ AU are: 10.0% of the set without Jupiter and 33.3% of the set with Jupiter. Thus, our model of the Galaxy relevantly changes the conventional result that ‘planetary perturbations do not significantly alter the perihelion distance’ (see, e.g., Dones et al. 2004, p. 161).

We have already mentioned that the above presented results hold for comets which still belong to long-period comets. Although nonnegligible part of comets was ejected from the Solar System due to the close encounter with Jupiter, the conventional statement that ‘only about 5% of the new comets are returned to Oort cloud distances of $10^4 - 10^5$ AU’ (Weissman 1979; Dones et al. 2004, p. 157) is not consistent with our numerical calculations. Our results show that most of the new comets are returned to the distances of $(10^4 - 10^5)$ AU.

If we use the least-square fit of the form $N(< q) = C q^{2/3}$, where q is the perihelion distance and $N(< q)$ is the number of comets with perihelion distances smaller than the value q , we obtain

$$\begin{aligned} N(< q) &= C q^{2/3}, \quad q < 100 \text{ AU}, \\ C &= (2.248 \pm 0.103) \text{ AU}^{-3/2}. \end{aligned} \quad (72)$$

The error of C is 4.6%, greater than the error obtained without the action of Jupiter.

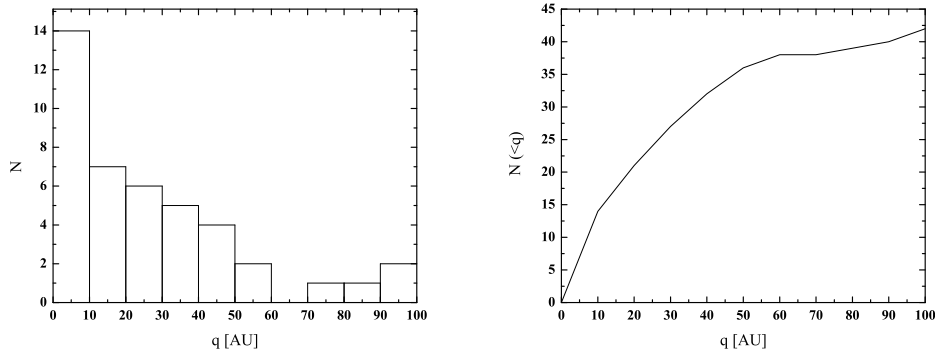


Fig. 11. Histogram and number $N(< q)$ of comets with perihelion distances smaller than the value q . Only cases for the inner part of the Solar System are depicted, $q < 100$ AU.

9.3. Distribution in ecliptical inclination

Fig. 12 depicts distribution in inclination with respect to the ecliptic. The action of Jupiter is marginal, although some difference between Figs. 6 and 8 exist. The isotropic distribution function (see Eqs. 5) of ecliptical inclination – inclination to the ecliptic – is in a good coincidence with the calculated data. However, 70% of the calculated orbits exhibit prograde orbits (ecliptical inclination is less than 90 degrees).

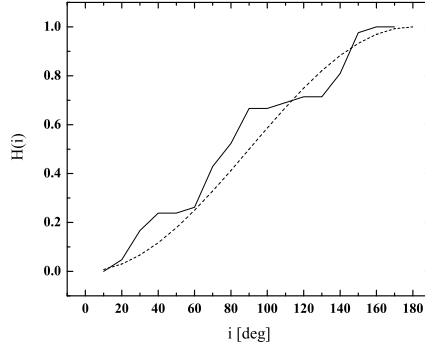


Fig. 12. Distribution function of cometary ecliptical inclination when comets are situated at their perihelia. Only cases for the inner part of the Solar System are depicted, $q < 100$ AU. The dotted line corresponds to the isotropic distribution.

One would await that gravity of a planet can influence the ecliptical inclination mainly in the cases when smaller perihelion distances occur. If the effect of the planet would not exist, then we should await no correlation between the perihelion distance and the ecliptical inclination. Our calculations show that the inclusion of Jupiter leads to the coefficient of correlation

$$r(q, i_{ecl}) = 0.366 \pm 0.135 . \quad (73)$$

The percentage probability that the correlation coefficient for the used set of data is greater than the given value is less than 2%.

10. Mass of the Oort cloud

Current estimates of the mass of the Oort cloud of comets are about (3.3 – 7.0) masses of the Earth (M_E), although the value of 38 M_E has also appeared (Dones et al. 2004, p. 162).

10.1. Observational data and the distribution function $F_a(a)$

Using observational data on the original semi-major axes of the long-period comets taken from Marsden and William's (1997) catalogue, we have found that the theoretical fit for the density function $f_a(a)$ in the exponential form a^α holds only for semi-major axes smaller than about 4×10^4 AU (see Fig. 13). Theoretical fit for the data, depicted in Fig. 13, yields for the distribution function

$$F_a(a) = \left(\frac{a}{a_0} \right)^{\alpha_{obs} + 1} , \quad a \leq a_0 ,$$

$$\alpha_{obs} + 1 = 1.133 \pm 0.044 \text{ AU} ,$$

$$a_0 = 4 \times 10^4 \text{ AU} . \quad (74)$$

Relative error of the exponent is 3.9%. Comparison with Eqs. (68) yields $a_{max} = a_0$, $a_{min} \rightarrow 0$. Eqs. (74) give that the observed density function of semi-major axis is

$$f_a(a) = \frac{\alpha_{obs} + 1}{a_0} \left(\frac{a}{a_0} \right)^{\alpha_{obs}} , \quad a \leq a_0 ,$$

$$\alpha_{obs} = \frac{4}{30} ,$$

$$a_0 = 4 \times 10^4 \text{ AU} . \quad (75)$$

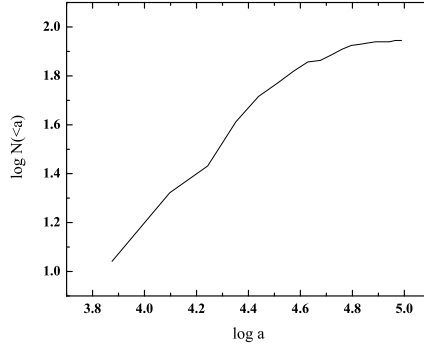


Fig. 13. Dependence of the cumulative number of long-period comets on semi-major axis a [AU] in logarithmic scale. The dependence is linear for $a < 4 \times 10^4$ AU.

If we would like to fit the curve in Fig. 13 up to $a = 1 \times 10^5$ AU using the approximation given by Eqs. (68), then

$$\begin{aligned} \alpha + 1 &= 0.449 \pm 0.049, \\ a_{min} &\rightarrow 0. \end{aligned} \quad (76)$$

We could fit the curve in Fig. 13 up to $a = 1 \times 10^5$ AU using the approximation given by Eqs. (68) with greater values of a_{min} . However, large errors of the exponent $\alpha + 1$ exist in these cases. For example, the value $a_{min} = 0.1 \times 10^5$ AU yields relative error of $\alpha + 1$: about 160%.

Let us calculate mean value of the semi-major axis. On the basis of Eq. (68) we can write

$$\begin{aligned} \langle a \rangle &= \int_{a_{min}}^{a_{max}} a' f_a(a') da' \\ &= a_{max} \frac{\alpha + 1}{\alpha + 2} \frac{1 - (a_{min}/a_{max})^{\alpha+2}}{1 - (a_{min}/a_{max})^{\alpha+1}}. \end{aligned} \quad (77)$$

Figure 14 depicts the value of $\langle a \rangle / a_{max}$ as a function of the exponent α for the cases found by various authors: $\alpha = -3/2$ (Duncan et al. 1987), $\alpha \in (-4, -2)$ (Fernández and Ip 1987, Fernández 1992, Fernández and Gallardo 1999). Also the value $\alpha = -0.55$ given by Eqs. (76) is considered. The value of $\langle a \rangle / a_{max}$ for the cases $\alpha = -3/2$ and $\alpha \in (-4, -2)$ are calculated under the assumption that $a_{min}/a_{max} = 0.1$ (see the solid curve and the square in Fig. 14). The case $\alpha = -0.55$ considers two possibilities, $a_{min}/a_{max} = 0.1$ (triangle in Fig. 14) and $a_{min} \rightarrow 0$ (star in Fig. 14). Our result represented by Eqs. (76) yields the value of $\langle a \rangle / a_{max}$ consistent with the value obtained from the model by Duncan et al. (1987). The case $\alpha = +1/2$ (Jeans 1919) yields more than two times greater value than the case $\alpha = -3/2$.

10.2. Number of comets in the Oort cloud

We will present two different accesses to the estimation of the number of comets in the Oort cloud. The first one is based on the comparison between the frequencies of cometary returns followed from the new physical model and the standard model of galactic tides. The second access considers the distribution of comets in the semi-major axis a when the density function is taken in the form proportional to a^α .

10.2.1. The first access

We have already mentioned the relevance of the physical model of the galactic tide (see Sec. 9.2 and the paper by Kómar et al. 2009). As a summary, we have that the number of oscillations of orbital elements is 10/6 times higher than for the standard model of the galactic tide (see Figs. 2 and 7 in

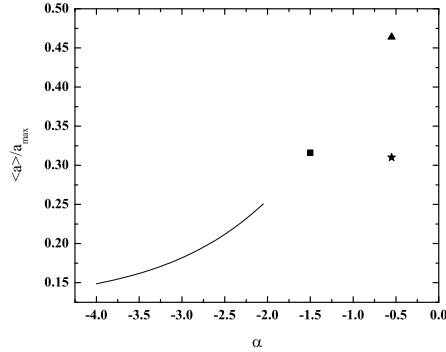


Fig. 14. The ratio of the mean value of semi-major axis to a_{max} as a function of the parameter α for various models. If $a_{min} / a_{max} = 0.1$, then the solid line corresponds to the model discussed by Fernández and Gallardo (1999), the square to Duncan et al. (1987), the triangle to $\alpha = -0.55$. The star corresponds to Eqs. (76) $\alpha = -0.55$ and $a_{min} \rightarrow 0$.

Kómar et al. 2009). On the basis of Sec. 9.2 we know that the number of comets coming to distances less than 5 AU is 28.6/5.0 times higher than it is in the standard model and the frequency of the returns may be even in 15/10 times greater (see Fig. 11). Thus we obtain that the number of occurrence of the long-period comets in distances less than 5 AU can be 15-times ($10/6 \times 15/10 \times 28.6/5.0 \doteq 15$) greater than the standard model offers (see, e.g., Dones et al. 2004, pp. 161-162).

10.2.2. The second access

On the basis of Eqs. (18) and Eqs. (77) we obtain that the ratio between the frequencies of cometary returns into the inner part of the Solar System for $\alpha = -3.5$, $a_{min} / a_{max} = 1/10$ (Dones et al. 2004, Fernández and Gallagher 1999) and $\alpha = -0.55$, $a_{min} \rightarrow 0$ (see Eqs. 76) is $f(0.55) / f(3.5) = (\langle a \rangle_{3.5} / \langle a \rangle_{0.55})^3 = 7$. On the basis of Sec. 9.2 we know that the number of comets coming to distances less than 5 AU is 28.6/5.0 times higher than it is in the standard model and the frequency of the returns may be even in 15/10 times greater (see Fig. 11). Thus we obtain that the number of occurrence of the long-period comets in distances less than 5 AU can be 60-times ($7 \times 15/10 \times 28.6/5.0 \doteq 60$) greater than the standard model offers (see, e.g., Dones et al. 2004, pp. 161-162).

10.2.3. Discussion

The two results were obtained, partially, in two different ways. The first case has not considered any density function in semi-major axis a . However, it was based on numerical calculations presented by Kómar et al. (2009) for $a = 5 \times 10^4$ AU, while more correct access is to use the mean value $\langle a \rangle$ as it is in the second case. In any case, both accesses yield values which are more than 10-times smaller than the conventional values (see, e.g., Dones et al. 2004).

10.3. Our estimate of the mass of the Oort cloud

On the basis of the results discussed above we can come to the conclusion that the mass of the Oort cloud is less than 0.5 mass of the Earth (maybe, even $0.1 M_E$). However, inclusion of perturbation by close stars and interstellar clouds may change the result.

We can present more exact calculation based on the above presented values. The current estimate of the mass of the Oort cloud of comets is (3.3 – 7.0) masses of the Earth (M_E), (Dones et al. 2004, p. 162), or $M' = (5.1 \pm 1.9) M_E$. Our two, partially independent, results yield that the real mass M is (15 – 60)–times smaller than the value M' , or, M is $d = (37 \pm 23)$ –times smaller than M' . Thus, $M = M' / d$. Using also error analysis, we finally obtain $M = (0.14 \pm 0.10) M_E$.

We have not considered the effect of nearby stars (interstellar clouds). Let the stars can generate N -times higher number of observable comets than the conventional/standard model of galactic tides offers. The real number of observable comets, due to the action of more realistic galactic tides, is $[(15-60) + N] / (1 + N)$ greater than the conventional estimate. Thus, the mass of the Oort cloud is $(1 + N) / [(15-60) + N]$ lower than the conventional estimate. The formula yields, as an example: $M \approx (1/20) M' \approx (1/4) M_E$ for $N = 1$, $M \approx (1/13) M' \approx (1/3) M_E$ for $N = 2$, $M \approx (1/7) M' \approx (5/7) M_E$ for $N = 5$, $M \approx (1/5) M' \approx 1 M_E$ for $N = 10$. If we take into account the result of Rickman et al. (2008, Fig. 2), then we should use, as an approximation, $N = 1$ (we remind that the authors use $\alpha = -1.5$ which significantly differs from 0).

11. Summary

The paper presents various results on the Oort cloud of comets if gravity of the Sun, Galaxy (and Jupiter in Sec. 9) are considered.

Sec. 2 discusses the (density) function of inclination. Besides the first theoretical part, the dominant part deals with the inclination with respect to the galactic equatorial plane. The important result shows that the exponent α , characterizing distribution of comets in the Oort cloud as a function of semi-major axis, should be equal to -1 if a_{min} corresponds to $(10 - 20) \times 10^3$ AU. This is not consistent with the cases treated in the literature (Duncan et al. 1987, Fernández and Ip 1987, Fernández 1992, Fernández and Gallardo 1999). If $a_{min} \ll (10 - 20) \times 10^3$ AU, then various values of α are admitted in our treatment of the distribution in inclinations.

Secs. 3 and 4 present simple relations for some dependencies. They both improve the published results and found new results. The relation between the semi-major axis a and oscillation period P is some kind of analogy to the third Kepler's law. The relation reads $a^3 P = 1$ if a and P are measured in natural units.

Sec. 6 seems to be of theoretical character. However, its results are applied to practical problems. One question remains open: Why various authors consider distribution in eccentricity in the form treated by Jeans (1919) as the relevant theoretical access but the other part of the Jeans distribution, corresponding to the density function for semi-major axis, is ignored? Results of Sec. 6 represented by Eqs. (66)-(67) are improvements of the published results (see e.g., Hills 1981, Fernández and Gallardo 1999). The result represented by Eq. (68) are used in Sec. 10.

Sec. 6 presents the effect of galactic tide to some observational quantities. The cumulative number of comets with perihelion distances is described by Eqs. (58) and (72), which can be generalized to the form $N(< q) = N(< q_0) (q/q_0)^{2/3}$, $q, q_0 \in (0, 100)$ AU. This is equivalent to the distribution function

$$F_q(q) = \left(\frac{q}{q_0} \right)^{2/3}, \quad q_0 = 100 \text{ AU}, \quad q \in (0, q_0). \quad (78)$$

This result differs from the conventional result based on the Jeans density function $f(e) = 2e$. However, if the authors do not agree with the Jeans density function of semi-major axis $f_a(a) \propto \sqrt{a}$, then they cannot use $f(e) = 2e$. Correspondingly, the distribution function cannot be of the form $F_q(q) = (q/a)(2 - q/a)$, as the authors state (see the second of Eqs. 52). More correctly, if one wants to use $f(e) = 2e$, he should be able to present an argument in favor of the choice and the argument must be independent of the argument presented by Jeans (1919). Moreover, the results of Sec. 6.4.3 show that $F_q(q) \propto q$ for the inner part of the Solar System holds for any density function of the form $f(e) = (k + 1)e^k$, $k > 0$, not only for $k = 1$.

Sec. 9 considers also the gravity of Jupiter. The gravitational action of Jupiter significantly influences the distribution in perihelion distance. The real number of long-period comets may be about 50-times smaller than the number conventionally considered, as it is discussed in Sec. 10.

We have already mentioned the problem with the values of the exponent α . The exponent characterizes the distribution of comets in the Oort cloud as a function of semi-major axis. We have found, in Sec. 2 for distribution in inclinations, that only the condition $a_{min} \ll (10 - 20) \times 10^3$ AU enables $\alpha \neq -1$. Sec. 10 deals with the value of the α in a different way. Sec. 10 comes to the conclusion that $\alpha = -0.55$ and $a_{min} \rightarrow 0$, see Eqs. (76). Secs. 6.3 and 9.2 yield $F_q(q) \propto q^{2/3}$ if also q greater

than several astronomical units are considered. If this holds also for $q > a_{min}$, then Eqs. (67) yields $\alpha = -1/3$. This is, approximately, consistent with the result of Eq. (76), $\alpha = -0.55$. Thus, we can conclude that α is about $-1/2$, more correctly, $\alpha \in (-0.6, -0.3)$.

Consideration of the results of the previous sections yields that mass of the Oort cloud of comets is (0.14 ± 0.10) masses of the Earth if the action of the nearby stars (galactic clouds) is negligible. The mass of the Oort cloud is less than $1 M_E$ even if the effect of the nearby stars is important.

12. Conclusion

The main results are:

1. Theoretical number of long-period comets with perihelion distance $q < 5$ AU is about 50-times greater than the conventional approach yields. (Gravity of Jupiter was taken into account in finding this result.) Mass of the Oort cloud of comets is, probably, about 1/4 mass of the Earth.
2. Semi-major axis a and period of oscillations P of eccentricity (and other orbital elements) are related as $a^3 P = 1$ in natural units for a moving Solar System in the Galaxy. The natural unit for time is the orbital period of the Solar System revolution around the galactic center and the natural unit for measuring the semi-major axis is its maximum value for the half-radius of the Solar System corresponding to the half-radius of the Oort cloud. The relation holds for the cases when comets approach the inner part of the Solar System, e.g., perihelion distances are less than ≈ 100 AU.
3. The minimum value of semi-major axis for the Oort cloud is $a_{min} \ll 1 \times 10^4$ AU. This condition was obtained both from the numerical results on cometary evolution under the action of the galactic tides and from the observational distribution of long-period comets. If the density function of semi-major axis is approximated by proportionality a^α , then α is, approximately, $-1/2$.
4. The magnitude of the change in perihelion distance per orbit, Δq , of a comet due to galactic tides is a strong function of semi-major axis a , proportional to $a^{8.25}$.

The usage of the density function of eccentricity in the form $f(e) = 2e$ cannot be argued to be the result obtained by Jeans (1919). Consequence of the Jeans calculations is marginal density function of semi-major axis proportional to \sqrt{a} and this is not consistent with the conventionally used distributions. Moreover, Figs. 7 and 8 in Kómar et al. (2009) show that gravitational tides alone would produce only values $e < 0.9$ for galactic inclinations i less than 90 degrees and practically $e < 0.8$ for $i \approx 90$ degrees: only for very short time intervals e is greater than 0.8 (e is close to 1 during the cometary visit of the inner part of the Solar System).

Using the observations yielding the distribution function of perihelion distance $F_q(q) \propto q$ (inner part of the Solar System), we cannot come to the conclusion that $f(e) = 2e$. Any density function of the form $f(e) = (k+1)e^k$, $k > 0$ is also consistent with the observational result $F_q(q) \propto q$.

Observational data on distribution in semi-major axis a , theoretical analytical results on the distribution functions $F_a(a)$ and of a perihelion distance, and, detailed numerical calculations on gravitational action of the Galaxy lead to a conclusion on $F_a(a)$. The conclusion is that approximation of $F_a(a)$ by the form proportional to $a^{\alpha+1}$ is consistent with all the mentioned methods if α is about $-1/2$.

The obtained results may be improved to be more accurate. This will require also more robust and more detailed numerical calculations (and, also, several planets, not only Jupiter, have to be considered).

Appendix A: Inclination with respect to the ecliptical plane

(Reference to equation of number (j) of this appendix is denoted as Eq. (A j). Reference to equation of number (i) of the main text is denoted as Eq. (i).)

We are interested in the inclination with respect to the ecliptical plane if we know inclination (and longitude of the ascending node) with respect to the galactic equatorial plane.

The transformation will be found in several steps.

We will use x_i , $i = 1, 2, 3$ (and also primed quantities for other reference frames, all with origin in the Sun) for coordinate right-handed axes. Summation convention is adopted, i.e. summation over repeated indices is assumed.

At first, we will find unit vector normal to the (osculating) orbital plane of the comet. Let the orbital plane is characterized with the ascending node Ω and galactic inclination i in the unprimed system. In order to obtain coordinates in the system where preferred plane is given by the orbital plane of the comet, we will make two transformations:

$$\begin{aligned} x'_i &= A_{ij} x_j , \\ A_{11} &= + \cos \Omega , \quad A_{12} = + \sin \Omega , \quad A_{13} = 0 , \\ A_{21} &= - \sin \Omega , \quad A_{22} = + \cos \Omega , \quad A_{23} = 0 , \\ A_{31} &= 0 , \quad A_{32} = 0 , \quad A_{33} = + 1 , \end{aligned} \tag{1}$$

and,

$$\begin{aligned} x''_i &= B_{ij} x'_j , \\ B_{11} &= + 1 , \quad B_{12} = 0 , \quad B_{13} = 0 , \\ B_{21} &= 0 , \quad B_{22} = + \cos i , \quad B_{23} = + \sin i , \\ B_{31} &= 0 , \quad B_{32} = - \sin i , \quad B_{33} = + \cos i . \end{aligned} \tag{2}$$

Eqs. (A1) and (A2) yield ($C_{ij} = B_{ik} A_{kj}$)

$$\begin{aligned} x''_i &= C_{ij} x_j , \\ C_{11} &= + \cos \Omega , \quad C_{12} = + \sin \Omega , \quad C_{13} = 0 , \\ C_{21} &= - \sin \Omega \cos i , \quad C_{22} = + \cos \Omega \cos i , \quad C_{23} = + \sin i , \\ C_{31} &= + \sin \Omega \sin i , \quad C_{32} = - \cos \Omega \sin i , \quad C_{33} = + \cos i . \end{aligned} \tag{3}$$

The inverse transformation is (transformation matrix C^T is inverse, in our case transpose, to the matrix C):

$$\begin{aligned} x_i &= C_{ij}^T x''_j , \\ C_{11}^T &= + \cos \Omega , \quad C_{12}^T = - \sin \Omega \cos i , \quad C_{13}^T = + \sin \Omega \sin i , \\ C_{21}^T &= + \sin \Omega , \quad C_{22}^T = + \cos \Omega \cos i , \quad C_{23}^T = - \cos \Omega \sin i , \\ C_{31}^T &= 0 , \quad C_{32}^T = + \sin i , \quad C_{33}^T = + \cos i . \end{aligned} \tag{4}$$

The unit vector normal to the orbital plane of the comet is characterized by the condition

$$(x''_1, x''_2, x''_3)^T = (0, 0, 1)^T . \tag{5}$$

Its galactic coordinates are, using Eqs. (A4),

$$\begin{aligned} \mathbf{e}_N &\equiv (x_1, x_2, x_3)^T , \\ x_1 &= + \sin \Omega \sin i , \\ x_2 &= - \cos \Omega \sin i , \\ x_3 &= + \cos i . \end{aligned} \tag{6}$$

The top of the vector \mathbf{e}_N is a point. The point has the following galactic coordinates

$$\begin{aligned} \mathbf{e}_N &\equiv (x_1, x_2, x_3)^T , \\ x_1 &= + \cos l \cos b , \\ x_2 &= + \sin l \cos b , \\ x_3 &= + \sin b , \end{aligned} \tag{7}$$

where l is the galactic longitude and b is the galactic latitude.

Comparison of Eqs. (A6)-(A7) yields

$$\begin{aligned} \cos l \cos b &= + \sin \Omega \sin i , \\ \sin l \cos b &= - \cos \Omega \sin i , \\ \sin b &= + \cos i . \end{aligned} \tag{8}$$

If Ω and i are given, then Eqs. (A8) offer

$$\begin{aligned}
b &= \arcsin(\cos i) , \\
\cos l &= + \frac{1}{\cos b} \sin \Omega \sin i , \\
\sin l &= - \frac{1}{\cos b} \cos \Omega \sin i .
\end{aligned} \tag{9}$$

We can easily find l from Eqs. (A9). It is sufficient to use the following prescription:

$$\begin{aligned}
\cos \Psi &\equiv C , \\
\sin \Psi &\equiv S , \\
S \geq 0 &\Rightarrow \Psi = \arccos C , \\
S \leq 0 &\Rightarrow \Psi = 2\pi - \arccos C .
\end{aligned} \tag{10}$$

We can summarize: We have i and Ω of a cometary orbit with respect to the galactic equatorial plane. The corresponding unit vector normal to the cometary orbit \mathbf{e}_N is given by Eqs. (A6). Galactic coordinates l and b of the unit vector are given by Eqs. (A7) and they can be found using Eqs. (A8)-(A10).

Equatorial coordinates of the vector \mathbf{e}_N are characterized by the right ascension α and the declination δ : $(\mathbf{e}_N \text{ eq.c.})_1 = \cos \alpha \cos \delta$, $(\mathbf{e}_N \text{ eq.c.})_2 = \sin \alpha \cos \delta$, $(\mathbf{e}_N \text{ eq.c.})_3 = \sin \delta$. Transformations between galactic and equatorial coordinates yield

$$\begin{aligned}
\sin \delta &= \sin b \sin \delta_0 + \cos b \cos \delta_0 \sin(l - l_0) , \\
\cos(\alpha - \alpha_0) \cos \delta &= \sin b \cos \delta_0 - \cos b \sin \delta_0 \sin(l - l_0) , \\
\sin(\alpha - \alpha_0) \cos \delta &= \cos b \cos(l - l_0) , \\
\alpha_0 &= 192.86^\circ , \\
\delta_0 &= 27.13^\circ , \\
l_0 &= 33.93^\circ .
\end{aligned} \tag{11}$$

If Ω and i are given, then Eqs. (A8)-(A11) enable to find α and δ . If $i = 0$, then $\delta = \delta_0$ and $\alpha = \alpha_0$.

Ecliptical coordinates of the vector \mathbf{e}_N are characterized by the ecliptical longitude λ and the ecliptical latitude β : $(\mathbf{e}_N \text{ ecl.c.})_1 = \cos \lambda \cos \beta$, $(\mathbf{e}_N \text{ ecl.c.})_2 = \sin \lambda \cos \beta$, $(\mathbf{e}_N \text{ ecl.c.})_3 = \sin \beta$. Transformations between equatorial and ecliptical coordinates yield

$$\begin{aligned}
\sin \beta &= \sin \delta \cos \varepsilon - \cos \delta \sin \varepsilon \sin \alpha , \\
\cos \lambda \cos \beta &= \cos \delta \cos \alpha , \\
\sin \lambda \cos \beta &= \sin \delta \sin \varepsilon + \cos \delta \cos \varepsilon \sin \alpha , \\
\varepsilon &= 23.5^\circ .
\end{aligned} \tag{12}$$

If Ω and i are given, then Eqs. (A8)-(A11) enable to find α and δ . If $i = 0$, then $\delta = \delta_0$ and $\alpha = \alpha_0$. If α and δ are known, then Eqs. (A10) and (A12) enable to find λ and β . If $\delta = 90^\circ$, then $\lambda = 90^\circ$ and $\beta = \arcsin(\cos \varepsilon)$.

Finally, the longitude of the ascending node Ω_{ecl} and the inclination i_{ecl} of the cometary orbit measured in the ecliptical coordinate system are given as follows:

$$\begin{aligned}
+ \sin \Omega_{ecl} \sin i_{ecl} &= \cos \lambda \cos \beta , \\
- \cos \Omega_{ecl} \sin i_{ecl} &= \sin \lambda \cos \beta , \\
+ \cos i_{ecl} &= \sin \beta .
\end{aligned} \tag{13}$$

The solution of Eqs. (A13) is

$$i_{ecl} = \arccos(\sin \beta) ,$$

$$\begin{aligned}
\sin \Omega_{ecl} &= + \frac{1}{\sin i_{ecl}} \cos \lambda \cos \beta, \\
\cos \Omega_{ecl} &= - \frac{1}{\sin i_{ecl}} \sin \lambda \cos \beta,
\end{aligned} \tag{14}$$

where also Eqs. (A10) must be used.

Appendix B: Motion of Jupiter in the ecliptical plane

(Reference to equation of number (j) of this appendix is denoted as Eq. (B j). Reference to equation of number (i) of the main text is denoted as Eq. (i).)

If we want to take into account also gravity of a planet, we need to find its position in the galactic coordinates. Let us consider Jupiter moving in a circular orbit in the ecliptical plane. Using results of the Appendix A, we can write for Jupiter coordinates

$$\begin{aligned}
x''_{1J} &= a_J \cos(\omega_J t + \varphi_0), \\
x''_{2J} &= a_J \sin(\omega_J t + \varphi_0), \\
x''_{3J} &= 0, \\
\omega_J &= \frac{2\pi}{a_J^{3/2}} yr^{-1}, \\
a_J &= 5.203 \text{ AU},
\end{aligned} \tag{1}$$

where t is the time and φ_0 is the arbitrary initial phase. The unit vector normal to the orbital plane of the comet is characterized by the condition

$$(x''_{1J}, x''_{2J}, x''_{3J})^T = (0, 0, 1)^T. \tag{2}$$

As for the galactic coordinates, we have (see Eqs. A6)

$$\begin{aligned}
(\mathbf{e}_N)_{gal} &\equiv (x_1, x_2, x_3)^T, \\
x_1 &= + \sin \Omega_J \sin i_J, \\
x_2 &= - \cos \Omega_J \sin i_J, \\
x_3 &= + \cos i_J.
\end{aligned} \tag{3}$$

Eqs. (A4) yield

$$\begin{aligned}
x_{1J} &= x''_{1J} \cos \Omega_J - x''_{2J} \sin \Omega_J \cos i_J, \\
x_{2J} &= x''_{1J} \sin \Omega_J + x''_{2J} \cos \Omega_J \cos i_J, \\
x_{3J} &= x''_{2J} \sin i_J.
\end{aligned} \tag{4}$$

We need the values of Ω_J and i_J .

We have $(\mathbf{e}_N)_{ecl} = (0, 0, 1)^T$. Transformations inverse to Eqs. (A12)

$$\begin{aligned}
\sin \delta &= \sin \beta \cos \varepsilon + \cos \beta \sin \varepsilon \sin \lambda, \\
\cos \alpha \cos \delta &= \cos \beta \cos \lambda, \\
\sin \alpha \cos \delta &= - \sin \beta \sin \varepsilon + \cos \beta \cos \varepsilon \sin \lambda, \\
\varepsilon &= 23.5^\circ,
\end{aligned} \tag{5}$$

yield for $\beta = 90^\circ$

$$\begin{aligned}
\sin \delta_J &= + \cos \varepsilon, \\
\cos \alpha_J \cos \delta_J &= 0, \\
\sin \alpha_J \cos \delta_J &= - \sin \varepsilon, \\
\varepsilon &= 23.5^\circ.
\end{aligned} \tag{6}$$

Solution of Eqs. (B6) is

$$\begin{aligned}\delta_J &= \arcsin(\cos \varepsilon) , \\ \alpha_J &= 270^\circ , \\ \varepsilon &= 23.5^\circ .\end{aligned}\tag{7}$$

Thus, we have

$$\begin{aligned}(e_N)_{eq} &= (\cos \alpha_J \cos \delta_J, \sin \alpha_J \cos \delta_J, \sin \delta_J)^T \\ &= (0, -\sin \varepsilon, +\cos \varepsilon)^T , \\ \varepsilon &= 23.5^\circ .\end{aligned}\tag{8}$$

As for transformation to the galactic coordinate system, we have to use transformations inverse to those represented by Eqs. (A11):

$$\begin{aligned}\sin b &= \sin \delta \sin \delta_0 + \cos \delta \cos \delta_0 \cos(\alpha - \alpha_0) , \\ \cos(l - l_0) \cos b &= \cos \delta \sin(\alpha - \alpha_0) , \\ \sin(l - l_0) \cos b &= \sin \delta \cos \delta_0 - \cos \delta \sin \delta_0 \cos(\alpha - \alpha_0) , \\ \alpha_0 &= 192.86^\circ , \\ \delta_0 &= 27.13^\circ , \\ l_0 &= 33.93^\circ ,\end{aligned}\tag{9}$$

which yield, together with Eqs. (B7),

$$\begin{aligned}\sin b_J &= \sin \delta_0 \cos \varepsilon - \cos \delta_0 \sin \varepsilon \sin \alpha_0 , \\ \cos(l_J - l_0) \cos b_J &= -\cos \alpha_0 \sin \varepsilon , \\ \sin(l_J - l_0) \cos b_J &= +\cos \delta_0 \cos \varepsilon + \sin \delta_0 \sin \varepsilon \sin \alpha_0 .\end{aligned}\tag{10}$$

Finally, we can write

$$\begin{aligned}(e_N)_{gal} &= (\cos l_J \cos b_J, \sin l_J \cos b_J, \sin b_J)^T \\ &= (\sin \Omega_J \sin i_J, -\cos \Omega_J \sin i_J, \cos i_J)^T .\end{aligned}\tag{11}$$

Eqs. (B10)-(B11) give

$$\begin{aligned}i_J &= \arccos \{ \sin \delta_0 \cos \varepsilon - \cos \delta_0 \sin \varepsilon \sin \alpha_0 \} , \\ \cos b_J &= \left\{ 1 - (\sin \delta_0 \cos \varepsilon - \cos \delta_0 \sin \varepsilon \sin \alpha_0)^2 \right\}^{1/2} \\ \cos(l_J - l_0) &= \frac{1}{\cos b_J} (-\cos \alpha_0 \sin \varepsilon) , \\ \sin(l_J - l_0) &= \frac{1}{\cos b_J} (\cos \delta_0 \cos \varepsilon + \sin \delta_0 \sin \varepsilon \sin \alpha_0) , \\ \sin \Omega_J &= +\frac{1}{\sin i_J} \cos l_J \cos b_J , \\ \cos \Omega_J &= -\frac{1}{\sin i_J} \sin l_J \cos b_J .\end{aligned}\tag{12}$$

Eqs. (A10) must be used in finding l_J and Ω_J .

Acknowledgement

This work was supported by the Scientific Grant Agency VEGA, Slovak Republic, grant No. 2/0016/09.

References

- Bailey M. E., 1983. The structure and evolution of the Solar System comet cloud. *Mon. Not. Roy. Astron. Soc.* **204**, 603-633.
- Dones L., Weissman P. R., Levison H. F., Duncan M. J., 2004. Oort Cloud formation and dynamics. In: Comets II. M. Festou, H. U. Keller and H. A. Weaver (Eds.), University of Arizona Press, Flagstaff, 153-174.
- Duncan M., Quinn T., Tremaine S., 1987. The formation and extent of the Solar System comet cloud. *Astron. J.* **94**, 1330-1338.
- Fernández J. A., 1992. Comet showers. In: Chaos, Resonance and Collective Dynamical Phenomena in the Solar System, Proc. IAU Coll. 152. S. Ferraz-Mello (Ed.), Kluwer Academic Publishers, Dordrecht, 239-254.
- Fernández J. A., Ip W.-H., 1987. Time-dependent injection of Oort cloud comets into Earth-crossing orbits. *Icarus* **71**, 46-56.
- Fernández J. A., Gallardo T., 1999. From the Oort cloud to Halley-type comets. In: Evolution and Source Regions of Asteroids and Comets, Proc. IAU Coll. 173. J. Svoreň, E. M. Pittich and H. Rickman (Eds.), Astron. Inst. Slovak Acad. Sci., Tatranská Lomnica, 327-338.
- Hills J. G., 1981. Comet showers and the steady-state infall of comets from the Oort cloud. *Astron. J.* **86**, 1730-1740.
- Jeans J. H., 1919. The origin of binary systems. *Mon. Not. R. Astron. Soc.* **79**, 408-416.
- Klačka J., 2009a. Galactic tide. arXiv:astro-ph/0912.3112
- Klačka J., 2009b. Galactic tide in a noninertial frame of reference. arXiv:astro-ph/0912.3114
- Kómar L., Klačka J., Pástor P., 2009. Galactic tide and orbital evolution of comets. arXiv:astro-ph/0912.3447
- Levison H. F., Dones L., 2007. Comet populations and cometary dynamics. In: Encyclopedia of the Solar System. L.-A. McFadden, P. R. Weismann and T. V. Johnson (Eds.), Elsevier (Academic Press), San Diego - London - Amsterdam - Burlington, second edition, chapter 31: 575-588.
- Marsden B. G., Williams G. V., 1997. Catalogue of Cometary Orbits 1997. Minor Planet Center, Smithsonian Astrophysical Observatory, Cambridge, MA, 12th Edition, 119 pp.
- Oort J. H., 1950. The structure of the cloud of comets surrounding the Solar System and a hypothesis concerning its origin. *Bull. Astron. Inst. Neth.* **11**, 91-110.
- Pástor P., Klačka J., Kómar L., 2009. Galactic tide and secular orbital evolution of comets. arXiv:astro-ph/0912.3449
- Rickman H., Fouchard M., Froeschlé Ch., Valsecchi G. B., 2008. Injection of Oort Cloud comets: The fundamental role of stellar perturbations. *Celest. Mech. and Dynam. Astron.* **102**, 111-132.
- Weissman P. R., 1979. Physical and dynamical evolution of longperiod comets. In: Dynamics of the Solar System. R. L. Duncombe (Ed.), Reidel, Dordrecht, 277-282.